Experiments concerning the mechanism of cytokinesis in *Caenorhabditis elegans* embryos

Dissertation

Zur Erlangung des akademischen Grades

Doctor rerum naturalium

(Dr. rer. nat.)

vorgelegt

der Fakultät Mathematik und Naturwissenschaften der Technischen Universität Dresden

von

Henrik Bringmann

Geboren am 15.1.1979 in Antony (Frankreich)

Erster Gutachter: Dr. Tony Hyman (MPI-CBG)

Zweiter Gutachter: Dr. Joe Howard (MPI-CBG)

Dritter (externer) Gutachter: Dr. Thomas Surrey (EMBL Heidelberg)

Eingereicht am: 05.09.06

Tag der Verteidigung: 10.01.07

Table of contents

Acknowledgements

Many people supported my PhD work. I am grateful for supervision, tutelage, technical help, insight into unpublished data, reagents, shared ideas, discussions, and moral support. All parts of this thesis work that relied on the help of others are indicated in the respective sections.

I gratefully acknowledge:

Tony Hyman, Joe Howard, Thomas Surrey, Petra Schwille, Frank Juelicher, Carrie Cowan, Stephan Grill, Alexander Zumdieck, Martin Srayko, Karen Oegema, Jon Audhya, Pierre Goenczy, Katy Afshar, Koen Verbruegghe, David Burgess, Bruce Bowerman, Morgan Goulding, Andra Zinke, Anne Schwager, Stefanie Schonegg, Jun Kong, Garrett Greenan, Laurence Pelletier, Conny Lorenz, Jeff Stear, Carsten Hoege, Tim Noetzel, Ronald Naumann, Alex Tudor Constantinescu, Christian Eckmann, Joanne Stamford, Alex Bird, Nurhan Otzlu, Jens Roper, Lesilee Rose, Theresa Stiernagle, Julie Ahringer, Andrei Posniakowsky, Susanne Ernst, Anne-Lore Schlaitz, the Caenorhabditis elegans genetics center, the MRC Genservice, the Koelle lab, the Boehringer Ingelheim Fonds, Cenix Bioscience.

Summary

In my thesis I aimed to contribute to the understanding of the mechanism of cytokinesis in *C. elegans* embryos. I wanted to analyze the relative contributions of different spindle parts – microtubule asters and the midzone - to cytokinesis furrow positioning. I developed a UV laser-based severing assay that allows the spatial separation of the region midway between the asters and the spindle midzone. The spindle is severed asymmetrically between one aster and the midzone. I found that the spindle provides two consecutive signals that can each position a cytokinesis furrow: microtubule asters provide a first signal, and the spindle midzone provides a second signal. The use of mutants that do not form a midzone suggested that the aster-positioned furrow is able to divide the cell alone without a spindle midzone. Analysis of cytokinesis in hypercontracile mutants suggests that the aster-positioned cytokinesis furrow and the midzone positioned furrow inhibit each other by competing for cortical contractile elements. I then wanted to identify the molecular pathway responsible for cytokinesis furrow positioning in response to the microtubule asters. To this end, I performed an RNAi screen, which identified a role for LET-99 in cytokinesis: LET-99 appeared to be required for aster-positioned cytokinesis but not midzone-positioned cytokinesis. LET-99 localizes as a cortical band that overlaps with the cytokinesis furrow. Mechanical displacement of the spindle demonstrated that the spindle positions cortical LET-99 at the site of furrow formation. The furrow localization of LET-99 depended on G proteins, and consistent with this finding, G proteins are also required for aster-positioned cytokinesis.

Introduction

Cell division

Reproduction of cells is essential to life. Cells usually reproduce by duplicating their contents and then dividing into two daughter cells. The cycle of duplication and division is called the cell cycle. The cell cycle culminates with the physical division of one cell into two daughter cells in a process called mitosis. Mitosis is characterized by a reorganization of the cytoskeleton that includes the formation of the mitotic spindle, a microtubule-based structure that controls cell division. An important function of the mitotic spindle is to segregate daughter chromosomes into two nuclei. In a process called cytokinesis, the cell physically cleaves into two cells. The position of the cytokinesis furrow determines the size and the content of the resulting daughter cells. The mitotic spindle positions the cytokinesis furrow midway between the poles of the mitotic spindle[1].

The mitotic spindle positions the cytokinesis furrow

The idea that the mitotic spindle positions the cytokinesis furrow has been extensively tested and verified over the last 100 years, primarily by using micromanipulation experiments[2]. The clearest demonstration is that if a spindle is mechanically displaced, the position of the furrow always coincides with the new position of the spindle. Rappaport confined sea urchin embryos in capillaries and mechanically displaced the spindle after the onset of furrowing. He

observed that the old furrow regressed and that a new furrow formed at the site of the spindle[3]. See figure 1. Further studies have tried to identify the spindle substructure that positions the furrow, primarily by assessing the sufficiency of various spindle parts to support furrowing. At the time of cytokinesis, the spindle consists of two microtubule asters connected together by a microtubule-based structure called the spindle midzone. The spindle midzone is a set of bundled non-kinetochore microtubules that forms between the chromosomes after chromosome segregation[2].

Researchers first hypothesized that microtubule asters position the cytokinesis furrow. The role of microtubule asters in furrow positioning was mainly investigated using mechanical manipulations in marine invertebrate embryos, such as sea urchin embryos.

For example Rappaport removed all parts of a mitotic spindle except one aster using a micropipette. The single aster moved to the center of the cell. He observed that a single aster cannot specify and ingress a cytokinesis furrow if the aster is positioned at the center of a cell. To generate an eccentrically positioned aster, Rappaport confined embryos in glass capillaries, see figure 2. He observed that a single aster can specify and ingress a furrow if it is eccentrically positioned[4].

However, evidence for a role of the spindle midzone in furrow specification also appeared. As an example, *Drosophila* geneticists identified a mutant, called *asterless*, that did not have detectable asters but still formed a spindle midzone. Mutant *asterless* cells formed and ingressed a cytokinesis furrow[5], see figure 2.

Numerous experiments in various systems have led to conflicting ideas: in some cells, the asters alone can specify a furrow, in others, the midzone alone can specify a furrow. One possibility to reconcile

the data is that different organisms and cell types use different mechanisms to position the cytokinesis furrow. An alternative possibility is that both asters and the midzone contribute to furrow positioning[6]. Recent work in *C. elegans* has implicated microtubule asters and the spinde midzone in cytokinesis[7, 8]. The best evidence for a role of microtubule asters in cytokinesis is that mutants with a disrupted spindle midzone can still specify a cytokinesis furrow[9-11].

The mitotic spindle positions the cytokinesis furrow at anaphase

Not only the positioning of the cytokinesis furrow is important for the correct segregation of cell contents but also the timing of cytokinesis. For instance, the cytokinesis furrow must form after sister chromatids have been separated. The mitotic stage while the sister chromatids are still attached to each other is called metaphase. At the next stage, called anaphase, sister chromatids are separated and move towards opposite spindle poles. The cytokinesis furrow typically ingresses at late anaphase[2]. A furrow might be positioned long before the furrow ingresses. When exactly is the position of the cytokinesis furrow first determined? To determine the time when the spindle establishes a furrow, the mitotic spindle was removed during different cell cycle times and furrow ingression was assessed. See figure 3. Hiramoto removed the spindle from sea urchin eggs by aspiration using a micropipette. If the spindle was aspirated away before or during metaphase, no cytokinesis furrow formed. If the spindle was removed at early anaphase before a cytokinesis furrow was visible, a cytokinesis furrow formed[12, 13]. This experiment

demonstrated that a furrow is not established before early anaphase. However, the furrow is established before a cytokinesis furrow becomes visible.

The role of the mitotic spindle in furrow ingression and completion of cytokinesis

Cytokinesis researchers hypothesized that the spindle plays a physical role not only for positioning but also for ingression of a cytokinesis furrow. However, classic data suggest that, at least in some systems, the spindle is dispensable for cytokinesis furrow ingression once it has initiated. For instance, Yatsu cut ctenophore eggs so that they contained the leading edge of the furrow but not the spindle. Although the cells did not contain spindles, the cleavage furrow still completed cytokinesis[14]. In another experiment, the spindle was aspirated away after specification, but before ingression, of the cytokinesis furrow in sea urchin eggs. In this experiment as well, the cytokinesis furrow completed[12, 13]. These experiments suggested that the mitotic spindle is dispensable for furrow ingression and completion of cytokinesis. Once initiated, the furrow is able to ingress without a spindle. In contrast to the micromanipulation data, genetic data has suggested that a part of the mitotic spindle, the spindle midzone, is required for the ingression of the furrow. This hypothesis is based on the observation that some mutants that do not form a spindle midzone form a cytokinesis furrow but fail to completely ingress this cytokinesis furrow, leading to a failure of cyotkinesis. This genetic data suggested an essential role of the spindle midzone for furrow ingression[9, 10].

Theories of cytokinesis furrow positioning

The nature of the cytokinesis furrow positioning signal from the spindle is unknown. It has been assumed that the spindle midzone could exert a positive signal that leads to furrow formation. The relatively small size of the midzone relative to the cell cortex could ensure a localized source of positional information. The nature of the spatial information provided by the astral signal, however, could either result from inhibition at the cell poles or stimulation between the asters. The model suggesting a negative signal is called polar relaxation and the model suggesting a positive signal is called equatorial stimulation.

Polar relaxation

White and Borisy initially proposed the polar relaxation model. The authors assumed that cytokinesis furrow formation is the consequence of increased cortical tension at the site of furrow formation. The model assumes that furrow contraction is caused by laterally mobile cortical contractile elements that are initially randomly distributed. The asters exert a negative signal to the cortex that repels cortical contractile elements from the poles and leads to the accumulation of cortical contractile elements between the asters. Thus the cortical tension on the poles is reduced and the cortical tension is increased between the asters, leading to the formation of a furrow[15]. In one version of this model, the negative signal from the asters was proposed to depend on the density of microtubules. According to this model the microtubule density would be lowest

between the asters, a result of the elongation of the spindle during anaphase[8].

Equatorial stimulation

Rappaport first proposed an equatorial stimulation model. In the equatorial stimulation model, asters contribute a positive furrow-promoting signal that directly induces a cytokinesis furrow. It was initially suggested that a change in the density of microtubules acts as a signal[2]. Another version of a equatorial stimulation model assumes the existence of a specific set of furrow-inducing microtubules that would be non-uniformly trafficked on the astral microtubules and would thus only induce a furrow at a specific site[16].

C. elegans as a laboratory organism

Caenorhabditis elegans is a free-living soil nematode that is approximately one millimeter long. It feeds on bacteria. Under laboratory conditions *C. elegans* is fed *Escherichia coli* bacteria grown on plates or in liquid culture. *C. elegans* has a rapid life cycle of approximately three days under laboratory conditions. *C. elegans* has two sexes: hermaphrodite and male. The two sexes differ in size, morphology and behavior. The sex typically used for laboratory experiments is the hermaphrodite. It produces both sperm and eggs, can self-fertilize and lays approximately 300 eggs. If mated with a male, a hermaphrodite can produce additional eggs. Males arise spontaneously with a low frequency, roughly 1/500. Males are used to maintain egg-laying and for genetic crosses[17].

C. elegans is anatomically simple and a hermaphrodite contains exactly 959 somatic cells. The genome of *C. elegans* is sequenced. It consists of 97 megabases and contains approximately 19000 predicted genes[18]. In systematic screens, all predicted genes have been silenced using RNAi[19-22]. About 2000 genes have so far been reported to be essential for viability of *C. elegans* (wormbase.org, 2006).

In the past years *C. elegans* one-cell embryos have appeared as a powerful model system to study cell division. *C. elegans* embryos offer the advantages of both an embryonic and a genetic model system. *C. elegans* provides relatively large, transparent eggs (50µm long and 30µm wide), which are well-suited for micromanipulations, and a rapid and invariant development, which allows for high-resolution analysis of mutant phenotypes. The time between the beginning of DNA condensations and the completion of furrow ingression is approximately 15 minutes. Mutagenesis-based genetics and RNAi are established procedures[23].

The first cell division of *C. elegans*

In *C. elegans*, mature oocytes are fertilized in the spermatheca of an adult hermaphrodite. Mature oocytes are arrested in meiosis I. Fertilisation by sperm triggers the completion of meiosis I and II. Three of the haploid products of meiosis are extruded from the egg as polar bodies. The remaining haploid pronucleus contributes the maternal chromosomes to the embryo. The sperm contributes the centrioles and a haploid pronucleus to the egg. The centrioles progressively mature into centrosomes. The embryo is initially

symmetric. A signal from the centrosomes then breaks the symmetry, leading to the formation of two cortical domains, an anterior domain and a posterior domain. The two domains are characterized by the localization of PAR proteins. Proteins such as PAR-2 only localize to the posterior domain, and proteins such as PAR-3 only localize to the anterior domain. After polarity is established, the maternal and the paternal pronucleus migrate towards each other. The paternal pronucleus is associated with the centrosomes. The two pronuclei meet in the posterior of the cell. The complex of the pronuclei and centrosomes then moves to the center of the cell and rotates so that the centrosomes are aligned onto the long axis of cell. The mitotic spindle then forms in the center of the cell. At anaphase, the spindle is displaced towards the posterior. A cytokinesis furrow forms between the asters and bisects the spindle midzone. The displacement of the spindle to the posterior generates a physical asymmetry in the daughter cells: the posterior cell (called P1) is smaller than the anterior cell (called AB)[23]. The first cell division of *C. elegans* is shown as a cartoon in figure 4.

Genes involved in *C. elegans* cytokinesis.

A prerequisite for a complete understanding of cytokinesis is an inventory of all proteins involved. In *C. elegans*, proteins have been identified by chemical mutagenesis screens, RNAi screens, and biochemical purification[20, 24, 25]. Here I divide known cytokinesis proteins into four phenotypic classes. The different phenotypic classes are shown as a cartoon in figure 5.

1. Proteins essential for actomyosin contractility. Without such proteins, cells cannot divide. Contractility is absent.

2. Proteins not essential for actomyosin contractility but that regulate contraction. Without such proteins, a cytokinesis furrow forms and ingresses but with altered kinetics.

3. Proteins required for the formation of a spindle midzone and for actomyosin contractility. Without such proteins, cells cannot form a spindle midzone and cannot complete cytokinesis. Some contractility is present.

4. Proteins required for formation of a spindle midzone but that are not required for actomyosin contractiliy. Without such proteins, cells cannot form a spindle midzone but can divide.

1. Proteins essential for actomyosin contractility.

Embryos depleted of class 1 proteins do not form a cytokinesis furrow and often don't form a contractile ring. This class includes the following proteins: the small GTPase RHO-1 and its RhoGEF (LET-21), which are thought to be at the top of a signaling cascade that regulates cortical contractility; nonmuscle myosin 2 (NMY-2), its regulatory light chain (MLC-4), and actin (ACT-1, ACT-2, ACT-3, ACT-4), which are part of the contractile ring; and a formin-like protein (CYK-1), a profillin-like protein (PFN-1), and a cofilin-like protein (UNC-60A), which are thought to regulate the assembly of a contractile ring[26, 27].

2. Proteins that regulate actomyosin contractility.

Embryos depleted of class 2 proteins usually form and ingress a cytokinesis furrow. However, the kinetics of formation and ingression of the furrow is changed. Proteins of this class either decrease or increase cortical contractility. MEL-11, a myosin light chain phosphatase regulatory subunit reduces cortical contractility. Depletion of MEL-11 leads to faster ingression of the furrow. Proteins such as ANI-1, an anillin-like protein, UNC-59 and UNC-61, two septin-like proteins and LET-502, a Rho-binding kinase, increase cortical contractility. Depletion of these proteins leads to a slower ingression of the furrow and occasional failure of cytokinesis. It is possible that some of these proteins actually belong to the class of genes strictly required for furrow formation and ingression but that available mutants or RNAi-mediated protein depletion only cause a partial phenotype[28-30].

3. Proteins essential for formation of a spindle midzone and for actomyosin contractiliy.

Proteins depleted of class 3 proteins do not form a spindle midzone and do not fully ingress a cytokinesis furrow. Proteins of this class either belong to the centralspindlin complex or to the aurora B complex. The centralspindlin complex consists of ZEN-4, a kinesin-like molecule, and CYK-4, a putative RhoGEF. The aurora B complex consists of aurora B, a kinase, and several regulatory subunits. Embryos depleted of these proteins do not form a spindle

midzone, they form a cytokinesis furrow, but the furrows fails to ingress completely. The extent of ingression varies among the class 3 mutants. Embryos depleted of aurora B also display a chromosome segregation defect.

The centralspindlin complex localizes to metaphase chromosomes. At anaphase the complex relocalizes to the central part of the spindle midzone (hence its name). Centralspindlin also localizes to the tip of the ingressing cytokinesis furrow. The aurora B complex localizes to metaphase chromosomes and relocalizes to the spindle midzone during anaphase. Because embryos depleted of these proteins lack a spindle midzone and do not ingress a cytokinesis furrow, it has been suggested that the spindle midzone is required for ingression of the cytokinesis furrow[9, 10, 31-33].

4. Genes required for formation of a spindle midzone but not required for actomyosin contractiliy.

This class contains one protein, SPD-1. Embryos depleted of SPD-1 do not form a detectable spindle midzone. However, these embryos ingress a cytokinesis furrow. This finding suggests that the spindle midzone is not strictly required for cytokinesis in *C. elegans* one-cell embryos[11].

Mechanical manipulations in *C. elegans*

Mechanical manipulations in *C. elegans* embryos are possible using either irradiation with highly focused UV laser light or using glass needles.

Irradiation with highly focused UV laser light

In these experiments, parts of the embryo are irradiated and thus destroyed using a highly focused UV laser beam. In this thesis the UV light is generated by an Nd:YAG laser with a wavelength of 354 nm and a pulse energy of 10uJ per pulse. The beam is focused to 1.5 µm. The energy provided by the UV laser light is thought to be able to induce breakage of chemical bonds. The sample can be moved using a motorized stage allowing irradiation of different regions of the embryo. In *C. elegans* UV laser beams have been used to kill entire cells, sever microtubules, ablate centrosomes, cut spindles in half, and fragment microtubule asters[34-38].

Manipulations using glass needles

Glass needles can be use to mechanically displace cellular structures such as the mitotic spindle. Mechanical manipulations using glass needles have been used extensively to study cytokinesis in marine invertebrate eggs. In *C. elegans*, mechanical manipulations are difficult because an eggshell surrounds the embryos. However, the eggshell is flexible and can be deformed by a needle. Glass needle-mediated manipulations have been used at the two-cell stage and later to remove blastomeres and to alter spindle and blastomere orientation[39, 40]. A Mechanical manipulation of spindle position has not been reported for *C. elegans* one-cell embryos; I have established this technique as part of this thesis.

Aims of my thesis:

In my thesis work I investigated how the mitotic spindle positions the cytokinesis furrow. I specifically addressed the following questions:

1. What are the relative contributions of microtubule asters and the spindle midzone to cytokinesis?

2. What is the role of the spindle midzone in cytokinesis furrow ingression?

3. How are the cytokinesis-promoting activities of microtubule asters and the spindle midzone coordinated?

4. What are the molecular mechanisms contributing to cytokinesis furrow positioning by microtubule asters and the spindle midzone? What are the proteins involved in this process?

Figures Introduction

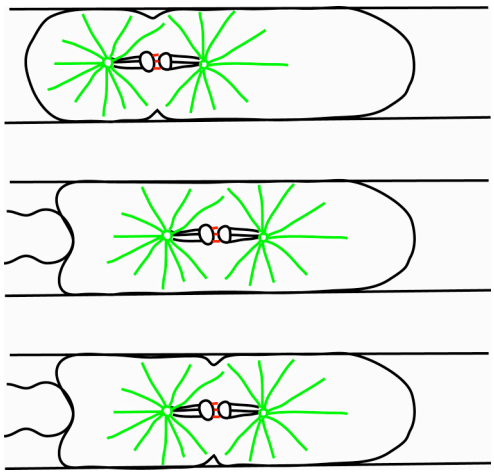

Figure 1: The mitotic spindle positions the cytokinesis furrow. Rappaport generated cylindrical cells by confining sea urchin eggs in capillaries. A furrow formed at the site of the mitotic spindle, midway between the asters (green) and directly over the spindle midzone (red). Rappaport moved the spindle with a blunt needle, which caused the furrow to regress. He then observed a new furrow at the site of the displaced spindle.

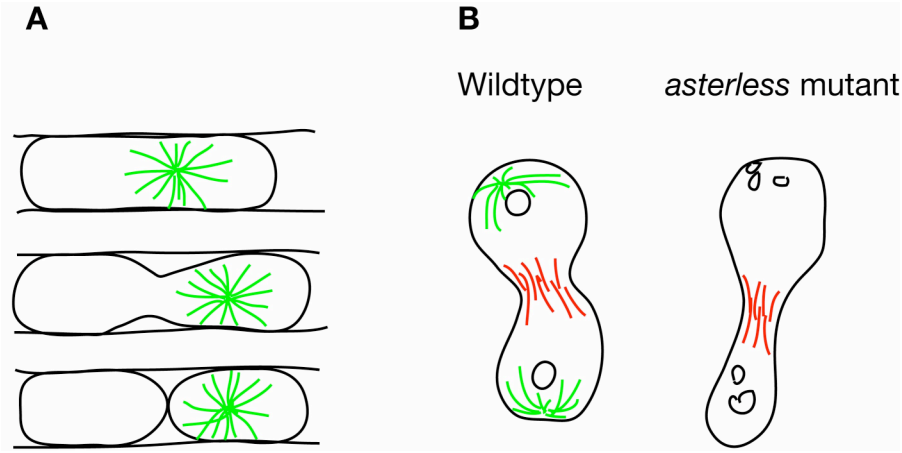

Figure 2: Microtubule asters or the spindle midzone alone can induce and position the cytokinesis furrow. Astral microtubules are shown in green, midzone microtubules are shown in red. **A** Rappaport removed most of the spindle but left a single aster in a sea urchin egg. He then confined the cells in a glass capillary and displaced the aster from the cell center. The single aster was able to induce a cytokinesis furrow when eccentrically positioned. **B** *Drosophila* geneticists identified a mutant called *asterless*. asterless mutants do not have detectable microtubule asters but can form a cytokinesis furrow.

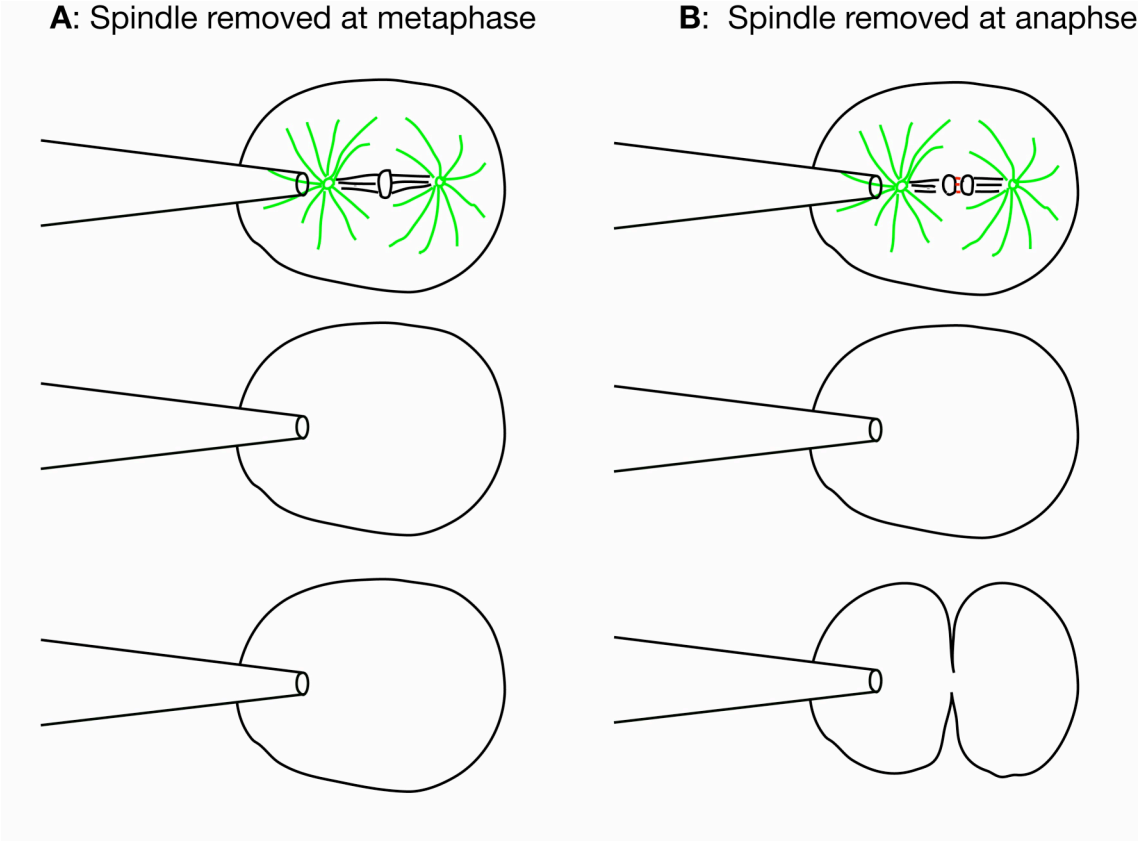

Figure 3: The mitotic spindle induces the cytokinesis furrow at anaphase, before visible ingression of the furrow. Once induced, a furrow can complete cell division without the mitotic spindle. Hiramoto aspirated away the spindle using a micropipette at different cell cycle stages. **A** If the spindle was removed before or at metaphase, no cytokinesis furrow ingressed. **B** If the spindle was removed at early anaphase, before a furrow ingressed or later, a furrow formed and completed despite the absence of a spindle.

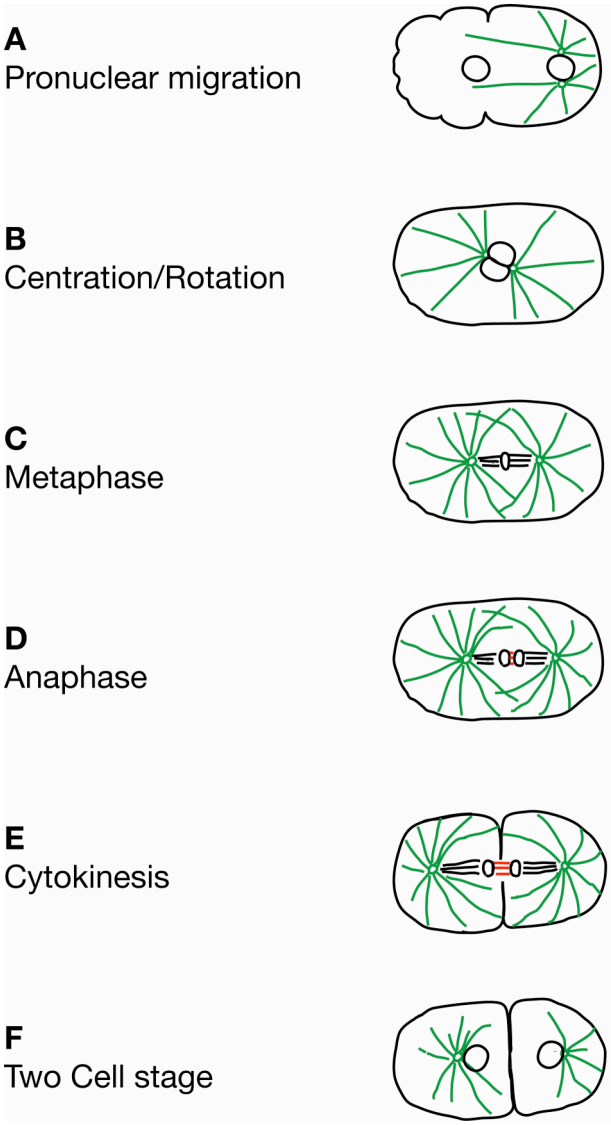

Figure 4: The fist cell division in *C. elegans* shown as a cartoon. Shown are the cell cortex (black), and the mitotic spindle (astral microtubules green, midzone microtubules red, spindle microtubule and nucleus/chromatin black).

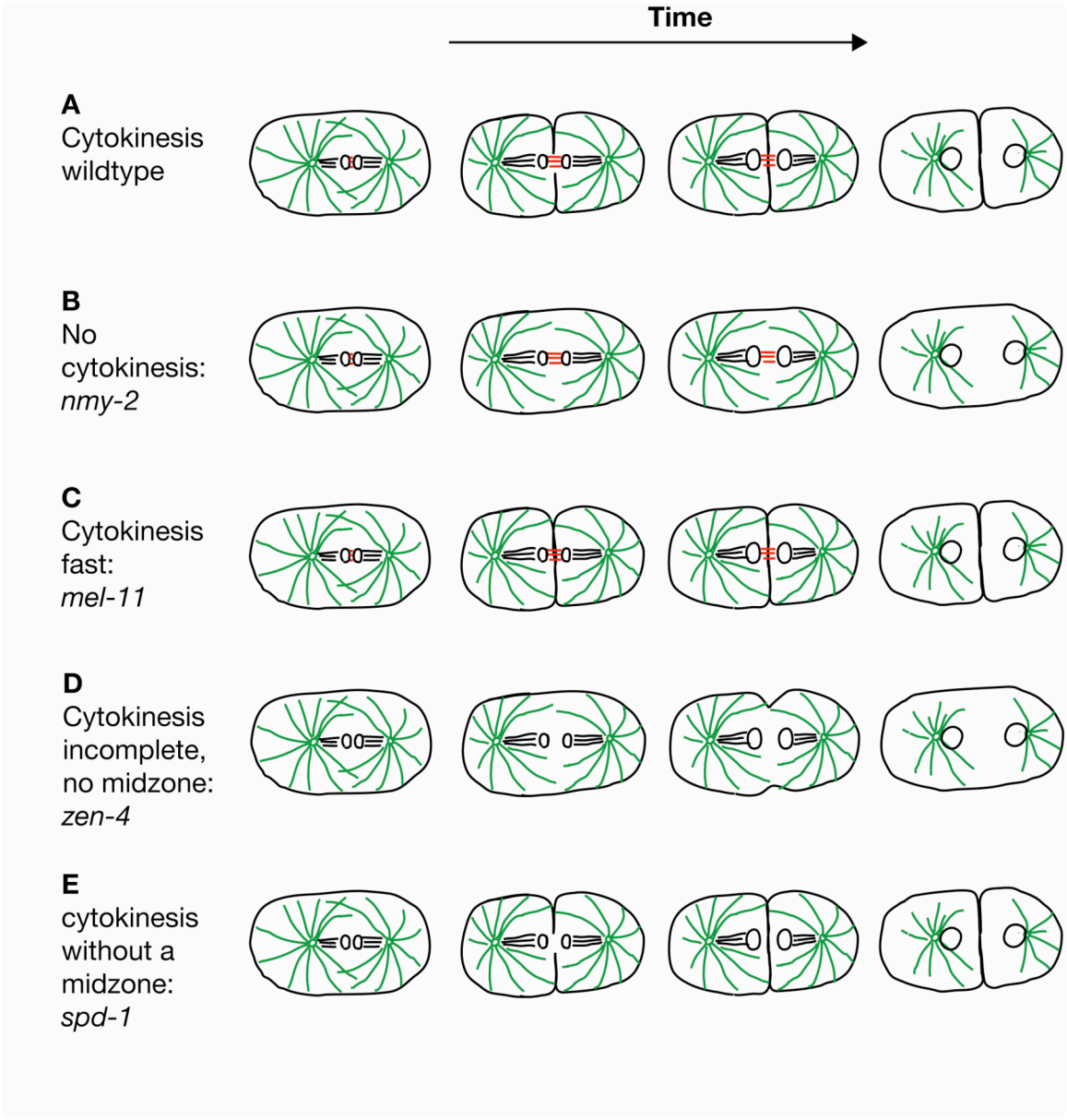
Time
A
Cytokinesis
wildtype
B
No
cytokinesis:
nmy-2
C
Cytokinesis
fast:
mel-11
D
Cytokinesis
incomplete,
no midzone:
zen-4
E
cytokinesis
without a
midzone:
spd-1

Figure 5

Figure 5: Genes involved in cytokinesis in *C. elegans* embryos. **A** Cartoon showing cytokinesis in wildtype. The cytokinesis furrow forms at the site of the mitotic spindle, midway between the spindle poles and at the site of the spindle midzone. **B** Depletion of proteins required for actomyosin contractility causes a complete absence of a cytokinesis furrow. **C** Depletion of proteins required for the regulation of actomyosin contractility cause a change in the kinetics of furrowing. For instance, a furrow can ingress faster compared with wildtype. **D** Depletion of proteins required for the formation of the spindle midzone and for contractility causes a defect in the completion of cytokinesis furrow ingression. **E** Depletion of proteins required specifically for the formation of the midzone does not cause a failure in cytokinesis.

Results and Discussion

1. What are the relative contributions of microtubule asters and the spindle midzone to cytokinesis?

Models

Microtubule asters and the spindle midzone have both been implicated in positioning the cytokinesis furrow. There are four extreme models as to how these two spindle substructures could contribute to furrow positioning. Two models assume a dominant mechanism and two assume a redundant mechanism: 1. Asters dominate positioning of the cytokinesis furrow; a midzone furrow would only contribute to furrow positioning if the astral signal was lacking. 2. The spindle midzone dominates positioning of the cytokinesis furrow; microtubule asters would only contribute to furrow positioning if the midzone signal was lacking. 3. Both the asters and the midzone contribute to one furrow-positioning signal. 4. Both the asters and the midzone provide independent signals. The problem with resolving these four models is determining the relative contributions from the two different parts of the spindle.

Problem and solution: symmetric and asymmetric spindles

The mitotic spindle is an inherently symmetric structure. A furrow-positioning cue from the asters would position the furrow midway between them. A midzone cue would position a furrow at the same place. In order to separate the contributions of the midzone and the asters to cytokinesis, the two structures must be spatially separated. A

spatial separation of the region midway between the asters and the spindle midway would occur in an asymmetric spindle in which one half-spindle is longer than the other. Such asymmetry would displace the midzone toward one side of the spindle and thus no longer positioned midway between the asters. Depending on the models presented above, I would expect the following results:

Model 1: If the asters dominate positioning the cytokinesis furrow, the furrow will form midway between the asters.

Model 2: If the spindle midzone dominates positioning the cytokinesis furrow, the cytokinesis furrow will form at the site of the spindle midzone.

Model 3: If both the microtubule asters and spindle midzone contribute to a single positional signal for cytokinesis furrow formation, the furrow will be positioned in some intermediate location.

Model 4: If both the microtubule asters and the spindle midzone contribute independent signals to position the cytokinesis furrow, one furrow will form midway between the asters and one furrow will form over the spindle midzone. The different models are shown as cartoons in figure 6.

Generating an asymmetric spindle

How can an asymmetric spindle be generated? In *C. elegans* first cleavage embryos, the mitotic spindle forms in the middle of the cell at metaphase. At anaphase, cortical pulling forces pull on the microtubule asters, separating the two spindle poles[37].

I took advantage of these pulling forces to design a UV-laser-based assay in which the position midway between the two asters was different from the position of the spindle midzone. The UV laser ablation set-up was built by Stephan Grill and was ready to use for my thesis work[38]. An embryo was observed using DIC microscopy until the onset of anaphase, the time at which the midzone forms. One aster was then separated from its associated chromatin using an ultraviolet laser, creating a cell with one isolated aster and the other aster still attached to the midzone. Cortical pulling forces moved the asters to opposite poles of the cell, positioning the spindle 'midzone' roughly one-third of the way along the aster-to-aster-distance (figure 7 and Supplementary movies 1, 2). Thus, the position of the midzone was different from the position midway between the two asters. I verified the change in spindle geometry using spinning disk imaging of YFP::alphatubulin and ZEN-4::GFP (see figure 7, the strains expressing YFP::alphatubulin and ZEN-4::GFP were gifts of Martin Srayko and Michael Glotzer, respectively). I termed this procedure asymmetric spindle severing (ASS). Following ASS, cytokinesis furrow ingression started midway between the asters. However, the furrow did not complete midway between the asters: the furrow paused and a second furrow formed at the cell cortex closest to the midzone (figure 7 and Supplementary movies 3–5). The two distinct furrows then met and cytokinesis completed, forming two cells. Thus, two furrows were observed after ASS, first a furrow between the asters and then a second furrow directed towards the midzone. Both furrows contributed to the final position of the cleavage plane.

Microtubule asters position the first furrow the spindle midzone positions the second furrow

Using cylindrical sea urchin embryos, it has been shown that the mitotic apparatus can induce multiple furrows if it is successively displaced along the long axis of the cell[3]. The experiment could be repeated up to 13 times in one embryo. Each time a new furrow formed, the old furrow regressed. Furthermore, a furrow can form after the mitotic spindle has been removed and before the onset of furrowing[12]. These experiments demonstrate that the furrow-inducing activity of the spindle is long-lived. It could thus be that the spindle midzone specifies both furrows, one before and one after its displacement. Alternatively, the asters may specify the first furrow while the midzone specified the second furrow. To resolve this problem, I compared cytokinesis furrow formation after anterior or posterior ASS: in anterior ASS, the spindle was severed at the anterior pole; in posterior ASS, the spindle was severed at the posterior pole. In both cases, the separated aster moved further to the pole of the cell compared with the aster that had the midzone attached. Thus, the position midway between the asters was different after anterior and posterior ASS, although the starting position of the midzone was the same. The difference in the mid-aster position is reflected in the difference in the position of the first furrow (see figure 7 and 8). After anterior ASS, the first furrow was positioned at 53.7 ± 0.9 % embryo length, but after posterior ASS, the first furrow was positioned at 56.5 ± 0.6 % embryo length (the difference is significant at the 0.05 level, $p = 0.041$, $N = 5$). After ASS, the position of the first furrow thus reflects the position of the asters.

As a further control of the ASS experiment I tried to find a condition in which the first furrow is located at a position that had never been in the vicinity of the spindle midzone. I found such conditions using monopolar spindles. Previous experiments have shown that either an isolated aster or a monopolar spindle is sufficient to specify a cleavage plane. In cells with a monopolar spindle, however, the cytokinesis furrow forms further away from the single aster compared to the normal position [16].

To generate monopolar spindles, I repeated ASS and subsequently disintegrated the separated aster using the UV laser (figure 8, supplementary movies 6 and 7). I verified that the aster was ablated using spinning disk imaging of YFP::alphatubulin. See figure 7. Under these conditions, the first furrow formed further away from the remaining aster compared to ASS with intact asters (ASS: 12.8 ± 0.2 μm, ASS plus aster disintegration: 18.0 ± 0.7 μm, N = 5). The position of the cytokinesis furrow following ASS plus aster disintegration was not related to the midzone position before ASS. The cleavage plane later re-directed towards the midzone. The spatial shift of the first furrow away from the intact aster indicates that the furrow position is not defined prior to spindle severing and is not determined by the midzone. Rather, the position of the first furrow appears to reflect the position of the microtubule asters. Taken together, these experiments suggest that a cytokinesis furrow is specified by two consecutive signals derived from distinct structures of the mitotic spindle: first, the microtubule asters and second, the spindle midzone.

2. Is the spindle midzone dispensable for cytokinesis furrow ingression?

Observations to be reconciled

Two phenotypic classes of spindle midzone mutants have reopened the debate as to whether the spindle midzone is required for cytokinesis furrow ingression:

1. Centralspindlin mutants display defects both in spindle midzone formation and in furrow ingression[9, 10].
2. The *spd-1* mutant displays a defect in spindle midzone formation but furrow ingression is normal[11].

At least two hypotheses can explain these observations:

1. The spindle midzone is required for cytokinesis furrow ingression but *spd-1* mutant cells do not completely lack the spindle midzone.
2. The spindle midzone is dispensable for cytokinesis furrow ingression, but centralspindlin mutants have an additional function in furrow ingression.

ASS analysis in spindle midzone mutants

To test these two hypotheses I first performed ASS in centralspindlin mutants. I measured furrow ingression depth as a function of time. If the centralspindlin mutants represent only a spindle midzone-null phenotype, the aster-positioned furrow should not be affected, but the midzone furrow should be absent.

I depleted the centralspindlin component ZEN-4 using RNAi-by-feeding. The feeding clone was a gift from Michael Glotzer. I tracked furrow ingression and plotted the ingression of the furrow versus

time. See figure 9. After ASS in *zen-4*(RNAi) embryos, the midzone-positioned furrow did not form, confirming the known role of centralspindlin in cytokinesis. In contrast, the aster-positioned furrow did form, but the aster-positioned furrow in *zen-4*(RNAi) ingressed less than the furrow in wildtype embryos: Maximum ingression of the aster-positioned furrow was 81 ± 3 % embryo width in wildtype embryos and 42 ± 4 % embryo width in *zen-4*(RNAi). N = 6.

This result suggests that ZEN-4 must have at least two roles: the known role in the formation of the midzone, and a second role in ingression of an aster-positioned furrow. Thus it seems unlikely that the *zen-4* mutant phenotype is not exclusively a "midzone null" phenotype. This result is consistent with the finding that ZEN-4 does not only localize to the spindle midzone but also localize to the ingressing furrow, and this furrow localization is independent of a detectable spindle midzone[11].

I then performed ASS in *spd-1*(*oj5*) mutants (a gift from Koen Verbrugghe). See figure 8. Again I measured furrow ingression as a function of time. After ASS in *spd-1*(*oj5*) embryos, the midzone-positioned furrow did not form but the aster-positioned furrow did form, similar to *zen-4* mutants. However, the aster-positioned furrow in *spd-1*(*oj5*) mutants ingressed twice as fast compared to wildtype cells (6 ± 1μm/s in wildtype embryos and 11 ±1μm/s in *spd*-1(*oj5*) embryos, n=5). Unlike in wildtype cells after ASS, the aster-positioned furrow did not pause but instead completed.

These observations suggest that the defective midzone in *spd-1(oj5)* is not able to specify a furrow, supporting the idea that the *spd-1(oj5)* mutant is a "midzone null" in terms of furrow positioning. The aster-positioned furrow in *spd-1* mutants is able to ingress completely, suggesting that the midzone is not essential for cytokinesis. Although

spd-1(oj5) worms seem to display a midzone-null phenotype it does not mean that they also display a *spd-1* null phenotype. It is possible that *spd-1* null cell would also have a cytokinesis phenotype.

3. How do the aster-positioned and midzone-positioned furrows interact?

Why does the aster-positioned furrow pause in the presence of the midzone?

If both the midzone and the asters can specify a cytokinesis furrow, why does a cell divide into two cells rather than three after ASS? Completion of two furrows is prevented because the aster-positioned furrow pauses and incorporates into the midzone-positioned furrow. The aster-positioned furrow can sometimes regress. Why does the aster-positioned furrow pause? A possible explanation is that the aster-positioned furrow does not complete because the midzone inhibits the activity of the aster-positioned furrow. The strongest piece of evidence supporting this idea is that in midzone-null (*spd-1*(*oj5*)) embryos, the aster-positioned furrow ingresses to completion at twice the speed of wild type embryos. This result suggests that the midzone exerts a negative effect on the aster-positioned furrow. In other words: the spindle midzone seems to inhibit the aster-positioned furrow.

How does the spindle midozone inhibit the aster-positioned furrow?

Rappaport generated cylindrical sea urchin eggs and moved the spindle to a new location after the furrow began to ingress. He observed that the old furrow regressed and a new furrow formed. Thus, although the cytokinesis furrow can complete in the absence of a spindle, the furrow will regresses if there is a competing furrow that receives continued or stronger stimulation [3, 12]. These experiments demonstrate that furrow positioning is very dynamic and can respond to the changing position of the spindle signal.

How does competition between furrows occur? In the astral relaxation model, White and Borisy suggested that cortical contractile elements with a high degree of cortical mobility increase the precision of cytokinesis furrow positioning. Control of the flow of contractile elements would determine the position of the furrow[15]. One likely explanation for why the aster-positioned furrow does not complete is that the aster-positioned furrow and the midzone-positioned furrow compete for a limited number of mobile contractile elements in the cortex . In this model, the aster-positioned signal would first recruit contractile elements, and the furrow would form and begin to ingress. The midzone-positioned furrow, specified slightly later, would also start recruiting contractile factors, thus competing with the aster-positioned furrow for cortical contractile elements. The aster-positioned furrow stops ingressing and either regresses or is incorporated into the midzone-positioned furrow. This model assumes that the midzone-positioned signal would eventually get stronger and outcompete the aster-positioned signal. This increase in signaling “strength” from the midzone might result from temporal regulation of the signals: the aster-mediated signal turns on earlier than the midzone-mediated signal and it might also turn off earlier.

One way to test this model would be to increase the amount of contractility in the cortex and then examine the competition between the two furrows. *mel-11* encodes a myosin phosphatase that antagonizes contraction caused by myosin light chain phosphorylation[28]. Loss of MEL-11 activity, in theory, would lead to more contractility, and consistent with this, *mel-11(it26)* mutant embryos undergo cytokinesis twice as fast as wild type embryos[28]. I thus performed ASS in *mel-11(it26)* mutant embryos and analyzed the kinetics of furrow ingression, as described above. See figure 9.

After ASS in *mel-11(it26)* mutants, both the aster-positioned furrow and the midzone-positioned furrow were formed. The aster-positioned furrow ingressed faster than in wild type embryos and completed, similar to midzone-null (*spd-1*(*oj*5)) embryos. The progression of the aster-positioned furrow was 6 ± 1μm/s in wildtype embryos and 11 ± 2μm/s in *mel-11*(*it26*) embryos (n=3). The midzone-positioned furrow also formed and completed in *mel-11*(*it26*) embryos. The *mel-11(it26)* embryos thus divided into three cells following ASS: one cell contained one aster, but no nucleus; one cell contained one aster and one nucleus; and one cell contained only a nucleus.

These observations are consistent with the hypothesis that contractility is limited in the embryo, thereby allowing competition between the aster-positioned furrow and the midzone-postioned furrow.

Other mechanisms are of course possible and could explain the observations equally well. For instance, the midzone could actively inhibit the aster-positioned signal. In this model, the *mel-11* phenotype could be explained by the fact that the aster-positioned

furrow ingresses fast enough to complete before the spindle midzone can actively inhibit the aster-positioned furrow.

4. Molecular mechanisms of cytokinesis

Both the microtubule asters and the spindle midzone can induce a cytokinesis furrow. If the midzone is defective, the aster-positioned cytokinesis furrow forms and the cell divides, but the midzone-positioned cytokinesis furrow does not form. Thus, cells can cleave efficiently without a spindle midzone, as occurs in *spd-1*(*oj5*) mutants, described above. My results using asymmetric spindle severing suggested, but did not prove, that cells could divide without aster-positioned cytokinesis.

The molecular mechanisms by which microtubule asters and the spindle midzone position the cytokinesis furrow are unknown. In order to understand cytokinesis furrow positioning at a molecular level, the molecules that define these two distinct pathways must be identified.

Based on previous results I would expect three classes of genes required for cytokinesis. 1) Genes required generally for cytokinesis; 2) genes required for aster-positioned cytokinesis; 3) genes required for midzone-positioned cytokinesis. Genes required generally for cytokinesis are components of the actomyosin contractile machinery, as discussed in the introduction. The centralspindlin complex also appears to be more of a general cytokinesis complex, as both aster-positioned and midzone-positioned furrows appear to be affected in *zen-4* mutants (see above). The only gene known to be required specifically for midzone-positioned cytokinesis is *spd-1*. In embryos

lacking SPD-1, a spindle midzone does not form and thus no midzone-positioned cytokinesis can occur. Genes required for aster-positioned cytokinesis have not been identified.

An RNAi screen to identify genes required for aster-positioned cytokinesis

To identify genes required for aster-positioned cytokinesis, Carrie Cowan and I performed an RNAi-based screen. We screened for genes required for cytokinesis only in the absence of a spindle midzone. A wild-type embryo will divide in the absence of a midzone, because the aster-positioned furrow is sufficient for cytokinesis. Thus, an embryo defective in aster-positioned cytokinesis will not cleave in the absence of a midzone. To facilitate the screening process, we disrupted the spindle midzone genetically using *spd-1*(*oj5*) mutant embryos. Because *spd-1*(*oj5*) mutants have no midzone, they have no midzone-positioned cytokinesis furrow but can cleave because they have an aster-positioned cytokinesis furrow[11]. We looked for genes whose depletion by RNAi prevented the embryo from cleaving specifically in a *spd-1*(*oj5*) mutant background but allowed the embryo to cleave in a wild-type background. Figure 10 A shows a cartoon description of the screen.
We silenced the gene function of approximately 1000 embryonic lethal genes using RNAi-by-feeding in wild type and *spd-1*(*oj5*) mutant worms (see materials and methods). All feeding clones for the screen were purchased from MRC Geneservice, Cambridge, England. Embryos were microscopically examined for multinucleated cells, which often result from failed cytokinesis. Gene disruptions that caused multinucleated embryos in *spd-1*(*oj5*) but not wildtype worms

were further observed to determine whether the multinucleate phenotype was indeed caused by a cytokinesis failure.

Of the 1000 genes screened, 60 produced a multinucleated phenotype in *spd-1*(*oj5*) and wild-type. Silencing of seven genes produced multinucleated cells only in a *spd-1*(*oj5*) background, and for three of these seven genes, the multinucleate phenotype resulted from a failure in cytokinesis. The three genes were *cls-2*, *gpr-1/2*, and *let-99* (See supplementary table).

These data suggest that in the absence of a spindle midzone, CLS-2, GPR-1/2, and LET-99 are required for cytokinesis, suggesting that these proteins may contribute to aster-positioned cytokinesis.

LET-99 is required for cytokinesis in the absence of a spindle midzone.

LET-99 is a DEP domain protein, which localizes to the cortex in a band, and has been implicated in controlling microtubule-based pulling forces involved in spindle positioning[41, 42]. In this study, I investigated the function of LET-99 in cytokinesis, a previously undescribed role for this protein.

To confirm that the cytokinesis failure in *let-99*(RNAi);*spd-1*(*oj5*) embryos was due to the spindle midzone defect seen in *spd-1*(*oj5*) mutants and not another role of *spd-1*, I analyzed cytokinesis furrow formation in *let-99* mutants with a mechanically disrupted spindle midzone.

I filmed embryos expressing alphatubulin::YFP by spinning disk microscopy to visualize both the spindle midzone and the asters of the mitotic spindle. (fig 10B). During early anaphase, after the onset of chromatid separation and the appearance of the spindle midzone, I

irradiated the midzone using a UV laser. As a result of irradiation, the two half spindles moved apart due to cortical pulling forces acting on the astral microtubules[37]. As shown in figure 10B, midzone disruption using a laser did not prevent the formation of a cytokinesis furrow, consistent with the idea that the spindle midzone is dispensable for furrow completion in one-cell *C. elegans* embryos. I confirmed that the laser light had indeed disrupted the midzone by looking for ZEN-4::GFP fluorescence, which localizes to the spindle midzone, after disruption of the midzone. ZEN-4::GFP was not detectable after laser ablation (data not shown).

I then used midzone ablation to study cytokinesis furrow formation in *let-99* mutant embryos. Non-irradiated *let-99*(RNAi) embryos formed a clearly visible spindle midzone and completed cytokinesis (see figure 10B). After midzone ablation in *let-99*(RNAi) embryos, the cortex showed shallow ingressions over the entire surface (see figure 10B). However, these ruffles did not ingress and cytokinesis failed. In the second mitotic cycle, embryos typically formed a tetrapolar spindle with midzone-like structures and cleaved (data not shown).

I conclude that LET-99 is required for aster-positioned cytokinesis. Laser ablation of the spindle midzone can phenocopy the *spd-1*(*oj5*) mutant phenotype indicating that the cytokinesis defect observed in the *spd-1*(*oj5*) *let-99*(RNAi) double mutant is caused by the spindle midzone defect described for this mutant[11].

LET-99 is dispensable for midzone-positioned cytokinesis

LET-99 is essential for aster-positioned cytokinesis. But is LET-99 dispensable for midzone-positioned cytokinesis? RNAi is unlikely to

provide a complete depletion of LET-99. Therefore I isolated a *let-99* null allele, using PCR to screen an EMS mutagenized *C. elegans* library. Alex Tudor Constantinescu and the lab of Christian Eckmann generated the EMS mutagenized *C. elegans* library. I screened the library using nested PCR (see materials and methods): Primers were selected to amplify the N terminus of LET-99. A deletion in this region would result in a PCR product that is smaller that the wildtype product. I obtained an N-terminal deletion, *let-99*(*dd17*). *let-99(dd17*) is likely to be a null because the N-terminus of the gene including the start codon and the DEP domain are deleted (see fig. 10 C and materials and methods).

All *let-99*(*dd17*) embryos examined completed cytokinesis (25/25). When I ablated the spindle midzone and observed embryos by time-lapse DIC microscopy, all *let-99*(*dd17*) embryos (15/15) showed small ingressions over the entire cortex but failed to form a cytokinesis furrow (see figure 10 C and compare supplementary movies 13-16). Additionally, a conditional *let-99* mutant, provided by Bruce Bowerman, *let-99*(*or204ts*), produced the same result as *let-99*(*dd17*) (Data not shown).

Thus, *let-99* is required specifically for aster-positioned cytokinesis; *let-99* is not required for midzone-positioned cytokinesis. *let-99* mutant embryos undergo cytokinesis in the presence of a midzone but fail to cleave in the absence of a midzone. These results emphasize that embryos can cleave without a spindle midzone, but that in the absence of a midzone, the aster-positioned cytokinesis furrow is essential. Conversely, *let-99* mutant embryos demonstrate that embryos can cleave without the aster-positioned furrow, but that in the absence of the aster signal, the midzone-positioned cytokinesis furrow is essential. In summary, either the aster-dependent or

midzone-dependent signal is sufficient for cytokinesis in one-cell *C. elegans* embryos; cells lacking both signals, however, fail to cleave.

Decreased aster separation is not the cause of the cytokinesis defect observed in LET-99 depleted embryos

It has been suggested that the separation of asters influences cytokinesis furrow ingression[2]. It has specifically been proposed that the increase of aster separation that occurs during anaphase is critical for asters to signal to the cortex[8]. Midzone ablation has been shown to increase aster separation[8, 11, 37]. I thus tested whether the cytokinesis defect that was observed after midzone ablation in LET-99 depleted embryos was a direct consequence of reduced aster separation.

I measured the separation of asters at the time of cytokinesis furrow formation. In wild-type embryos without midzone ablation, the two asters were separated by 43.8 ± 0.6 % embryo length. After UV laser-mediated midzone ablation, the asters were separated by 52 ± 3 % embryo length. Thus, aster separation is increased after mechanical midzone ablation in wildtype *C. elegans* embryos, in agreement with previous studies. I next investigated the effect of LET-99 depletion on aster separation. In *let-99*(*dd17*) embryos without midzone ablation, the two asters were separated by 38 ± 1 % embryo length, slightly less than wildtype embryos. In *let-99* mutant embryos after UV laser-mediated midzone ablation, the asters were separated by 45 ± 3 % embryo length. N = 5 for each experiment. Thus, while midzone ablation increases aster separation, LET-99 depletion reduces aster separation. However, the reduced spindle elongation in *let-99* mutants combined with the increased spindle elongation

resulting from midzone ablation compensate each other: Aster separation is not significantly different in wildtype embryos containing a midzone compared with *let-99* mutant embryos in which the midzone is ablated. (44 ± 1 and 45 ± 3 embryo elongation for wildtype and *let-99*(*or204ts*) respectively). Because aster separation in *let-99* mutant embryos under my experimental conditions is not significantly different from aster separation in wildtype embryos, it seems unlikely that the cytokinesis defect observed after midzone ablation in LET-99 depleted embryos is caused by a variation in aster separation.

To further support this idea, I tried to find conditions in which aster separation is reduced but cytokinesis takes place in the absence of a spindle midzone. I thus compared two different *let-99* alleles: *let-99*(*or204ts*) and *let-99*(*or513ts*). Bruce Bowerman and Morgan Goulding provided the two unpublished alleles. Midzone ablation in *let-99*(*or204ts*) embryos caused a failure in cytokinesis furrow ingression. Midzone ablation in *let-99*(*or513ts*) embryos did not cause a failure in cytokinesis furrow ingression (data not shown). However, both embryos have the same degree of aster separation (45 ± 3 and 43 ± 1% embryo length for *let-99*(*or204ts*) and *let-99*(*or513ts*), respectively). N = 5 for each experiments. Thus, the decreased aster separation in *let-99* mutants is not related to the cytokinesis defect seen following midzone ablation.

LET-99 contributes to contractile ring formation and the timing of cytokinesis.

During cytokinesis, signals from the mitotic spindle reorganize the acto-myosin cortex, leading to the formation of a contractile ring[2]. I

wanted to look at the role of LET-99 in the kinetics of contractile ring contraction. The contractile ring can be visualized using fluorescently-tagged nonmuscle myosin 2 (NMY-2::GFP)[29, 43]. The traditional view of a contractile ring from the side of an embryo makes it difficult to examine ring morphology. Therefore I imaged embryos end-on: individual embryos were transferred to a glue-coated coverslip and turned onto their posterior pole using a micromanipulator-controlled glass needle (see materials and methods). The embryos were imaged using spinning disk microscopy, and I calculated the rate of ring closure from time-lapse movies. NMY-2::GFP was concentrated at the leading edge of the ring in *let-99* mutants as well as in wild-type. The rate of ring contraction was similar in *let-99* mutant and wildtype embryos (0.52 ± 0.03 % embryo diameter per second (N = 5) for wildtype and 0.59 ± 0.03 % embryo diameter per second (N = 5) in *let-99*(*or204ts*) embryos). However, the contractile ring in *let-99* mutant embryos was irregularly shaped, compared to wildtype embryos in which the contractile ring is circular. Furthermore, after the ring had ingressed, I observed ectopic furrows in *let-99* mutant embryos, which often caused cytoplast formation (Figure 11 A-B).

I also examined the role of LET-99 in the timing of cytokinesis furrow formation by imaging NMY-2::GFP embryos conventionally from the side from metaphase until the completion of cytokinesis. I found that the furrow formed later in *let-99* mutant embryos compared with wildtype embryos (wildtype 84 ± 2 s after anaphase onset; *let-99*(*dd17*) 155 ± 8 s after anaphase onset, n=5; (Figure 11 C).

Although reduced aster separation in *let-99* embryos is unlikely to account for their failure to form a cytokinesis furrow folloing

midzone ablation, I wondered whether aster separation might influence the kinetics and morphology of the contractile ring. To test whether the altered contractile ring formation and ingression in *let-99* mutant embryos is caused by reduced aster separation, I measured the timing of cytokinesis in cells with one aster. To generate cells with only one aster, ASS plus aster disruption was carried out using the UV laser, as described above. After ASS plus aster disruption in wildtype embryos, the first furrow formed at a position away from the remaining aster and away from the spindle midzone. The second furrow formed over the position of the spindle midzone. The first furrow formed 100 ± 7s after anaphase onset; the second furrow formed 353 ± 19s after anaphase onset. After ASS plus aster disruption in *let-99*(*dd17*) embryos, multiple furrows appeared all over the cortex. However, usually only one of these furrows ingressed and completed. The ingressing furrow was always directed at the spindle midzone. The single ingressing furrow formed 153s ± 8s after anaphase onset, later than the aster-dependent furrow but earlier than the midzone-dependent furrow in wildtype embryos. N = 6 for each experiment. Thus, *let-99* mutant embryos with one aster have a similar delay in the onset of cytokinesis furrow ingression as *let-99* mutant embryos with two asters. Thus, these results indicate that the late onset of furrowing in *let-99* mutant embryos is not caused by the reduced aster separation observed in these embryos.

One possible explanation for the late formation and the inhomogeneity of the contractile ring in the midzone-only cytokinesis embryos is that microtubules of the asters are touching and evenly distributed over the cortex, while the spindle midzone is located in the center of the cell[2]. The direct contact between astral microtubules and the cortex might be more suitable for providing a

precise and homogenous signal, which would be required for a regularly shaped ring. Furthermore, a midzone signal might take longer to reach the cortex compared with a direct signal from the asters. This idea may also explain why the aster-positioned signal seems more prominent in the large blastomeres of early embryos[6]. However other explanations are possible, such as different cell cycle control of the two signals. In ASS experiments, I showed that the midzone-positioned furrow forms several minutes after the aster-positioned furrow. However in *let-99* mutants that lack the astral signal, the furrow forms only about one minute later than in wildtype. A possible explanation for the difference in timing of the midzone-positioned furrow after ASS and in *let-99* mutants is that there is competition between the two furrows: the aster-positioned furrow may inhibit formation of the midzone-positioned furrow. In the absence of an aster-positioned furrow, the midzone-positioned furrow might therefore form earlier.

LET-99 localizes to the site of cytokinesis furrow formation.

I next wondered whether the localization of LET-99 corresponds to its role in cytokinesis. Previous work using immunostaining of endogenous LET-99 has shown that LET-99 is enriched in a cortical band slightly posterior of the cell middle[42]. However the relationship between band formation and cytokinesis had not been studied. For this purpose, I needed transgenic embryos expressing a LET-99 fused to a fluorescent protein. The transgenic strains were constructed under my supervision by Jun Kong. He used both YFP (YFP::LET-99) and mCherry (mCherry::LET-99). The YFP vector

was a gift from Andrei Posniakowsky and the mCherry vector was a gift from Karen Oegema and Jon Audhya. Both constructs were tested by Jun Kong for functionality and rescued known *let-99* mutants (see materials and methods).

I recorded time-lapse images of YFP::LET-99 embryos from metaphase to the completion of cytokinesis (compare fig. 12 A). Confirming previous observations, LET-99 appeared as a cortical band during the first cell division[42]. LET-99 localized as a broad cortical band at metaphase, where it remained until it narrowed around the ingressing furrow at anaphase. I quantified cortical LET-99 (YFP::LET-99) intensity as a function of embryo length (see materials and methods) (Figure 3). N = 20 cortices = 10 embryos. The localization was similar using both the fluorescent fusion constructs (YFP or mCherry, see materials and methods).

LET-99 distribution at metaphase peaked in the middle of the cell (50 ± 1 % embryo length), and covered about 55% of the embryo surface (from 27 ± 2 % embryo length to 83 ± 1 % embryo length). At anaphase, the LET-99 band shifted to the posterior (56 ± 1 % embryo length), so that the peak LET-99 intensity now coincided with the position of the presumptive cytokinesis furrow (55 ± 1 % embryo length). LET-99 distribution narrowed slightly during anaphase, covering about 40% of the embryo surface (from 39 ± 2 % embryo length to 78 ± 1 % embryo length).

The time-lapse analysis of LET-99 suggests that LET-99 distribution is dynamic, with a significant change of overall distribution occurring during anaphase. The peak intensity of cortical LET-99 correlates with the site at which the cytokinesis furrow eventually ingresses, consistent with a role for LET-99 in cytokinesis.

The mitotic spindle positions cortical LET-99 at anaphase

At metaphase, the mitotic spindle is positioned roughly in the center of the cell. The analysis of the dynamics of LET-99 distribution showed that at metaphase, the band was localized imprecisely between the asters. At anaphase, both the spindle and the peak maximum were displaced toward the posterior. The band always localized precisely between the asters during anaphase, suggesting that the spindle may position the LET-99 band. To test this idea directly, I wanted to alter the position of the spindle and test whether the position of the LET-99 band also changed. I altered the position of the spindle using a glass needle and followed the localization of cortical YFP::LET-99 by time-lapse microscopy. I located embryos in late prophase or early prometaphase using DIC microscopy. I used a glass needle controlled by a micromanipulator to press orthogonally to the embryo's long axis, at approximately 60% embryo length. The pressure of the needle caused a slight displacement (around 5 to 10 microns) of the spindle away from the center of the cell. At anaphase, elongation of the spindle often increased the displacement away from the center. Posterior displacement that normally occurs during anaphase in one-cell *C. elegans* embryos was strongly reduced, resulting in two blastomeres of roughly equal sizes (see movie 16). Despite the lack of physical asymmetry at the two-cell stage, such embryos developed into fertile adults, showing that the manipulation did not interfere grossly with development.

I then analyzed YFP::LET-99 distribution following mechanical spindle displacement. From the beginning of the manipulation until

metaphase, the localization of the LET-99 peak was similar to unmanipulated cells and did not correlate with the position of the displaced spindle. At anaphase, cortical LET-99 moved towards the displaced spindle before furrow ingression was visible, and the LET-99 peak was positioned midway between the asters. The cytokinesis furrow formed at the site of the LET-99 peak, 20-30 seconds after repositioning of the LET-99 band. (See figure 12, N = 6 embryos for posterior spindle displacement and N = 8 embryos for anterior spindle displacement).

I thus conclude that before anaphase, a spindle-independent mechanism determines the cortical position of LET-99. During anaphase, the position of the mitotic spindle determines the cortical position of LET-99. This finding is consistent with the classic view that the cytokinesis furrow inducing signals are active at anaphase and not before[12].

Aster-positioned cytokinesis is independent of PAR polarity

What positions LET-99 before cytokinesis? LET-99 was initially described for its role in cell polarity. Cell polarity, as defined by the PAR proteins, is required for metaphase LET-99 band formation, and the position of the LET-99 band correlates with the boundary between anterior and posterior PAR domains[42]. Here I investigated the role for LET-99 in aster-positioned cytokinesis. I wanted to test whether aster-positioned cytokinesis is dependent on cortical PAR polarity. I thus ablated the spindle midzone in polarity defective embryos. The allele *par-3*(*it71*) contains an early nonsense mutation; it is likely to be a null allele and results in defective cortical

polarity[44, 45]. After midzone ablation in *par-3*(*it71*) embryos, all embryos divided successfully (5/5) (see figure 13). Thus cortical PAR polarity does not appear to be essential for aster-positioned cytokinesis. Consistent with this observation, the cortical LET-99 band during anaphase is not dependent on cortical polarity: A LET-99 band was also observed in polarity defective embryos[42]. Thus, the anaphase but not the metaphase LET-99 band appears to correspond to the function of LET-99 in cytokinesis.

LET-99 localizes to both the aster-positioned furrow and the midzone-positioned furrow

LET-99 is essential for aster-positioned cytokinesis but dispensable for midzone-positioned cytokinesis. LET-99 localizes to the site of cytokinesis furrow formation. I thus wondered whether LET-99 localizes to the aster-positioned cytokinesis furrow or the midzone-positioned cytokinesis furrow or both furrows. I thus performed ASS in embryos expressing YFP::LET-99. In order to increase the spatial separation of the two furrows, I ablated the severed aster ("ASS plus aster ablation", described above). I observed LET-99 localization using epifluorescence and quantified cortical YFP fluorescence, as described above. After ASS, YFP::LET-99 localization first peaked at the position of the aster-positioned furrow, away from both the remaining aster and away from the midzone. After several minutes YFP::LET-99 also localized to the cortex overlying the spindle midzone. YFP::LET-99 fluorescence peaked at the site of the presumptive midzone-posititioned furrow (see figure 14). Thus YFP::LET-99 localized to both the aster-positioned cytokinesis furrow and the midzone-positioned cytokinesis furrow. If LET-99 is

specifically required for aster-positioned cytokinesis but not for midzone-positioned cytokinesis, why does LET-99 localize to both furrows rather than only localizing to the aster-positioned cytokinesis furrow? Several explanations are possible: It is possible that the localization of the fluorescent fusion construct differs from the localization of the endogenous LET-99. However, this seems unlikely since the fluorescent fusion construct can rescue *let-99* mutants and the localization of the fluorescent protein is similar to published immunostainings of the endogenous protein[42]. An alternative explanation would be that LET-99 plays a role on the midzone-positioned furrow, but this role is not essential for furrow formation. Furthermore, LET-99 has been shown to be involved in additional processes such as spindle positioning and cortical polarity, and it is possible that the localization of LET-99 to the furrow reflects a function in a process unrelated to cytokinesis. It is also possible that LET-99 does not play a role on the midzone-positioned furrow but rather that this localization simply reflects a property of LET-99 to localize to furrows. This property could be essential for aster-positioned cytokinesis, but dispensable for midzone-positioned cytokinesis.

GOA-1/GPA-16 are required for LET-99 furrow localization

How does LET-99 localize to the cytokinesis furrow? My screen for genes that prevented formation of a cleavage furrow in the *spd-1* mutant background identified *gpr-1/2* as being potentially required for the aster-dependent signal. GPR-1/2 is a G protein regulator that acts through the redundant Galpha subunits GOA-1 and GPA-16[46,

47]. Previous results have shown that LET-99 and heterotrimeric G proteins act in the same pathway[48]. I therefore tested whether GOA-1/GPA-16 are involved in localizing LET-99 to the cytokinesis furrow. I depleted GOA-1/GPA-16 using RNAi-by-feeding in embryos expressing fluorescently labeled LET-99. The *goa-1/gpa-16* feeding clone was a gift from Katy Afshar and Pierre Gonczy. I filmed embryos using epifluorescence microscopy and quantified the cortical fluorescence intensity of mCherry::LET-99, as described above (see materials and methods). *goa-1*/*gpa-16*(RNAi) embryos formed a LET-99 band that was visible until metaphase/early anaphase. At the time of cytokinesis furrow formation, the cortical distribution of LET-99 appeared to be unrelated to the position of the cytokinesis furrow: I did not observe a strict enrichment of cortical LET-99 at the site of the cytokinesis furrow (Figure 15). Thus, the metaphase LET-99 band appears unaffected by *goa-1/gpa-16*(RNAi), but the anaphase LET-99 band was severely affected by *goa-1/gpa-16*(RNAi). A spindle-dependent mechanism positions the LET-99 band specifically at anaphase/cytokinesis. The enrichment of LET-99 at the cytokinesis furrow requires GOA-1/GPA-16. These results support the idea that two distinct LET-99 bands exist: one at metaphase and one at anaphase/cytokinesis. The two bands are positioned by different mechanisms and they appear to be molecularly distinct. The results further indicate that both LET-99 and the G protein pathway are involved in the same cytokinesis pathway, namely aster-positioned cytokinesis.

Figures Results

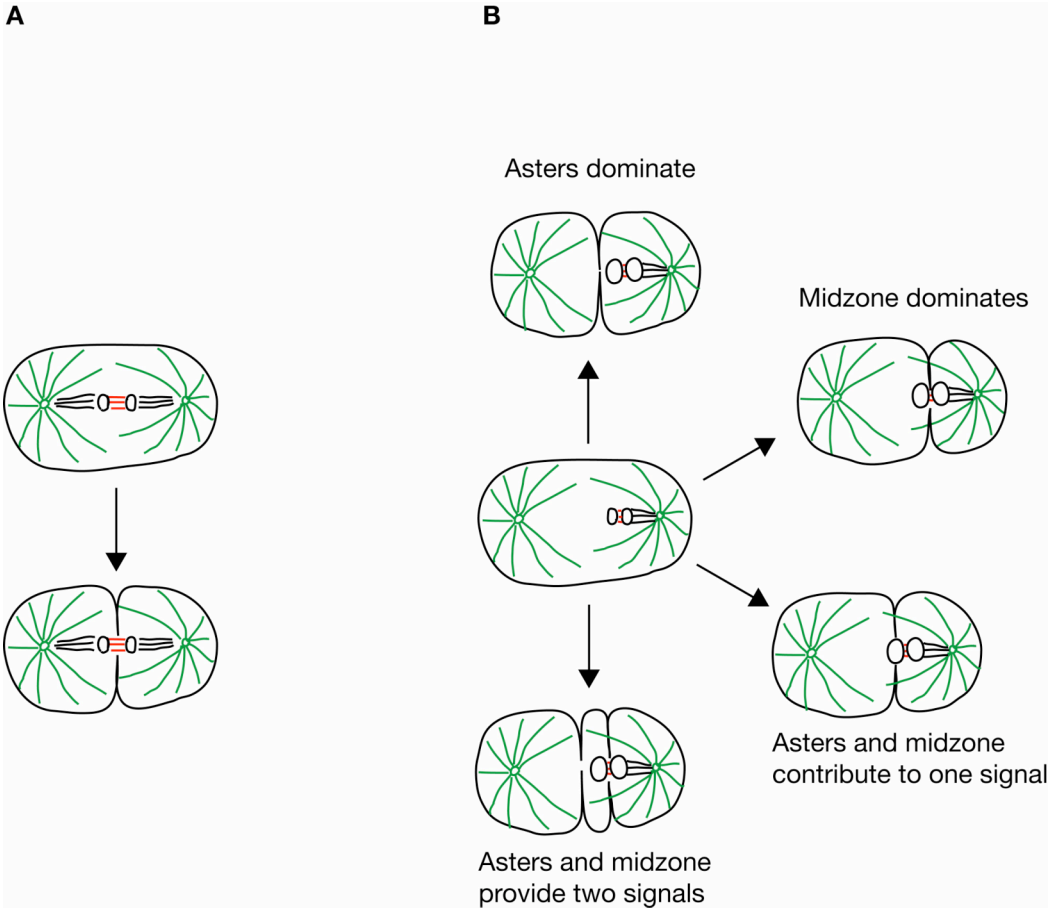

Figure 6

Figure 6: The relative contributions of microtubule asters and the spindle midzone can be studied in cells containing asymmetric spindles, in which the region midway between the asters and the spindle midzone are spatially separated. **A** A wildtype spindle is an inherently symmetric structure: A cue from the asters would position the furrow mid-way between them. The spindle midzone would position the furrow at the same place. **B** In order to separate the relative contributions of microtubule asters and the spindle midzone, the symmetry of the spindle must be broken so that the two structures are spatially separated. An asymmetric spindle could cleave in at least four different ways: The position of the furrow could be dominated either by the asters or by the spindle midzone, or the asters and the midzone could both contribute to furrow positioning. The two structures could either cooperate as one signal or act independently as two signals.

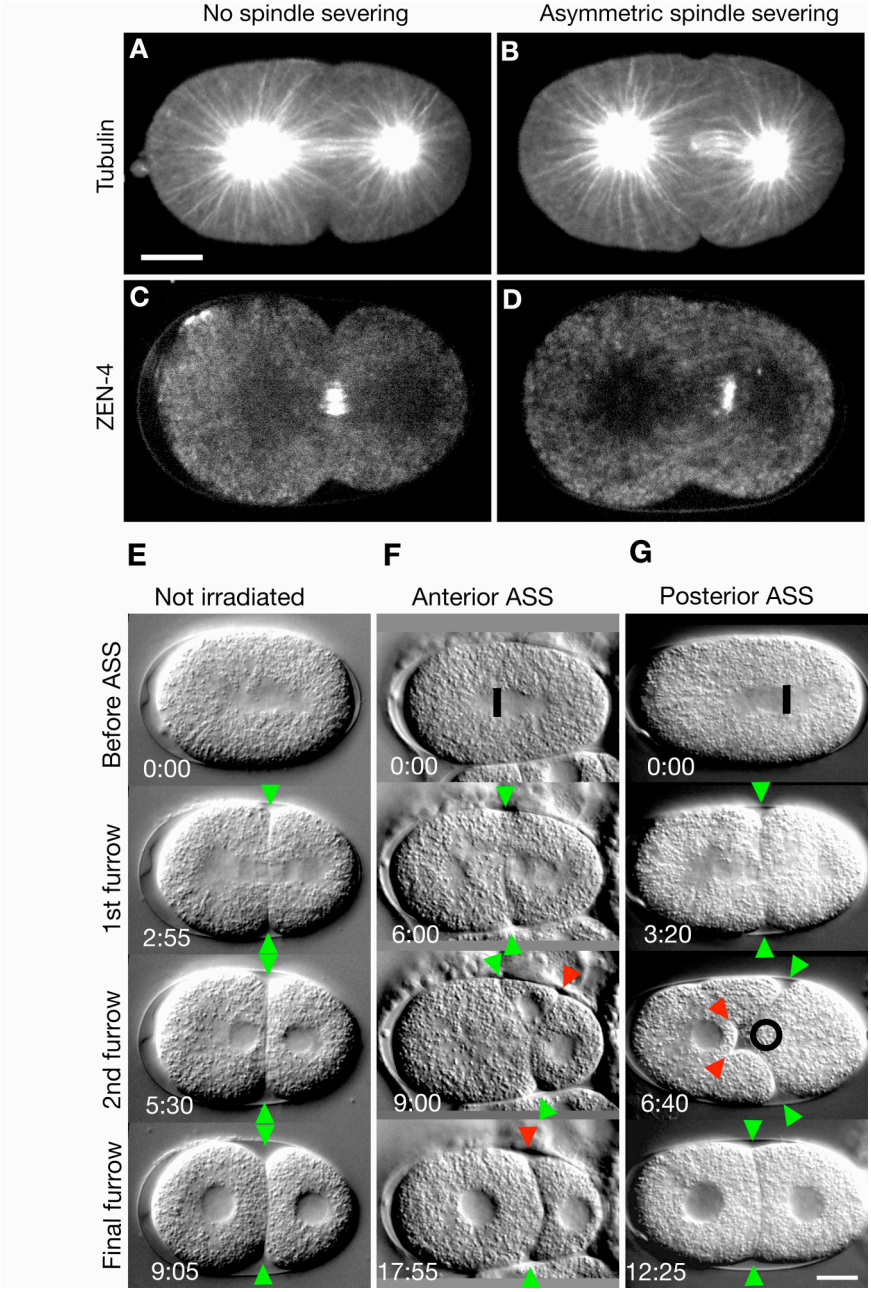
No spindle severing
Asymmetric spindle severing
A
B
C
D
Tubulin
ZEN-4
E
F
G
Not irradiated
Anterior ASS
Posterior ASS
Before ASS
1st furrow
2nd furrow
Final furrow
0:00
2:55
5:30
9:05
0:00
6:00
9:00
17:55
0:00
3:20
6:40
12:25

Figure 7

Figure 7: Asymmetric spindle severing (ASS) spatially separates the spindle midzone and the region midway between the asters, leading to the generation of two furrows. **A-D**, Alteration of spindle geometry: Spinning disk microscopy images after ASS performed in a YFP::α-tubulin background (**A-B**) and a ZEN-4::GFP background (**C-D**) to reveal the microtubule cytoskeleton and the spindle midzone, respectively. **A** and **C**, Unsevered control, **B** and **D**, severed spindle. **E-G**, Generation of two furrows after ASS: DIC microscopy image series (compare supplementary movies 1-5). **E**, Wild-type embryo, **F**, Separation of the anterior aster (A-ASS), **G**, Separation of the posterior aster (P-ASS). Black bar indicates irradiated region. The posterior nucleus lies outside of the focal plane in one image (position indicated by a black circle). Furrows were often unilateral after ASS. The asters seem to be attached to the ingressing furrow, which may cause the midzone to move off axis (see **F**). First furrows are indicated in green, second furrows in red. The difference in the furrowing after posterior and anterior ASS seems to be due to the geometry of the cell: After anterior ASS the midzone moves closer to the cortex compared with posterior ASS. In general, cytokinesis takes longer after ASS (roughly double the time compared to control). Posterior is to the right in **A-G** and scale bars are 10 μm.

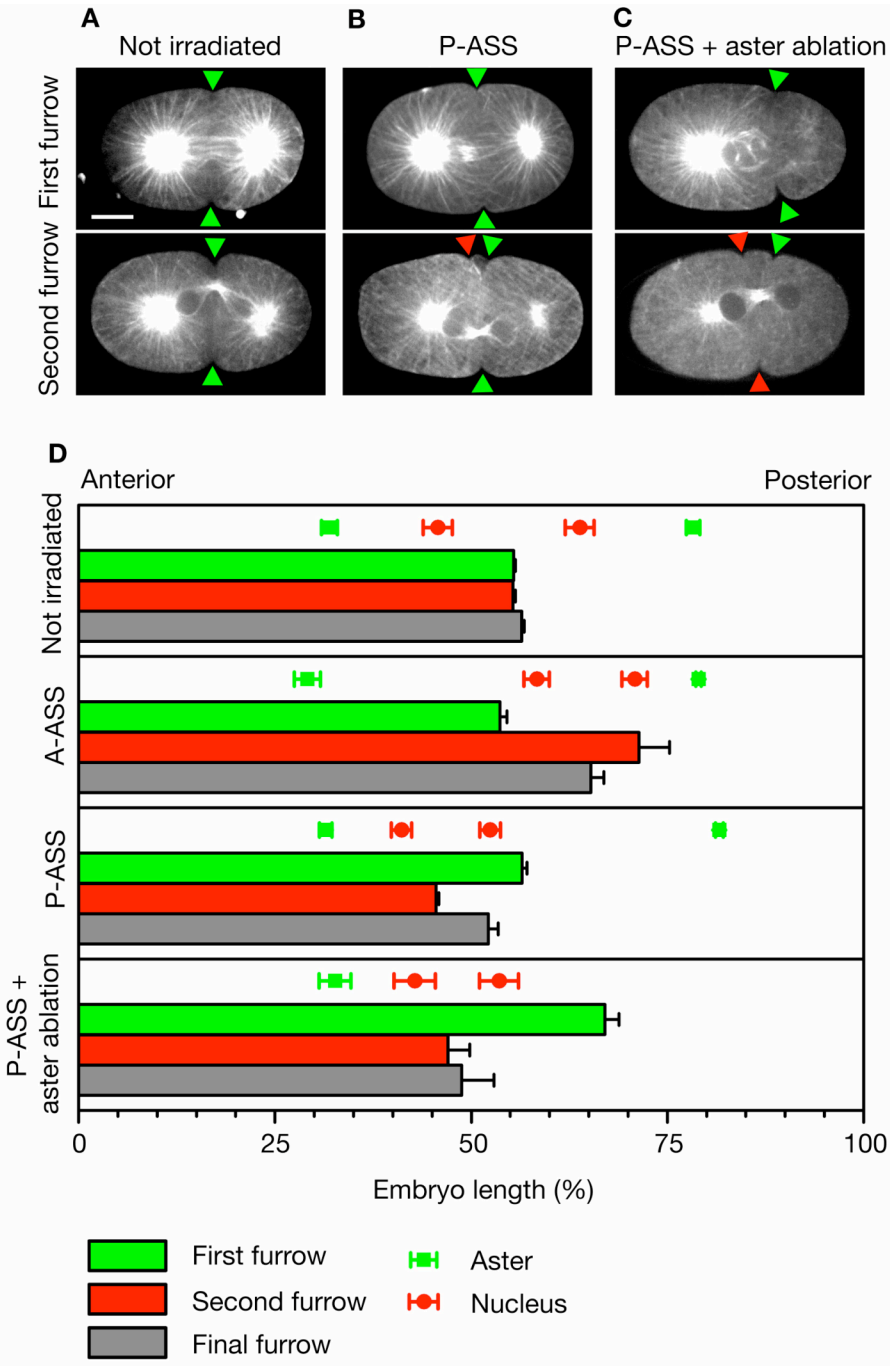
A
Not irradiated
B
P-ASS
C
P-ASS + aster ablation
First furrow
Second furrow
D
Anterior
Posterior
Not irradiated
A-ASS
P-ASS
P-ASS + aster ablation
0
25
50
75
100
Embryo length (%)
First furrow
Second furrow
Final furrow
Aster
Nucleus

Figure 8

Figure 8: Microtubule asters position the first cytokinesis furrow. The spindle midzone positions the second cytokinesis furrow. **A-C**, Spinning-disk microscopy snapshots after posterior ASS with and without subsequent aster ablation observed by YFP::α-tubulin fluorescence. **A**, Unsevered control. **B**, ASS **C**, ASS plus ablation of the severed aster. Embryos on top are shown at the time the first furrow (green arrowheads) ingresses. In **C**, the furrow sets up further away from the remaining aster compared with **A** and **B**. Embryos on bottom are shown at the time the second furrow ingresses. The second furrow (red arrowheads in **B** and **C**) always aims at the spindle midzone. Posterior is on the right. Scale bar, 10 μm. Compare supplementary movies 6 and 7 showing aster ablation in DIC microscopy. **D**, Quantification of spindle dimensions and furrow positions after ASS and ASS plus aster ablation: The position of the aster centres (green squares) and the nuclei (red dots) at the time the first furrow ingresses are indicated. The positions of the first (green), second (red), and final (grey) furrow are shown as histograms Shown are unsevered embryos, anterior and posterior ASS (A-ASS and P-ASS), and posterior ASS plus aster ablation. Errors are SEM.

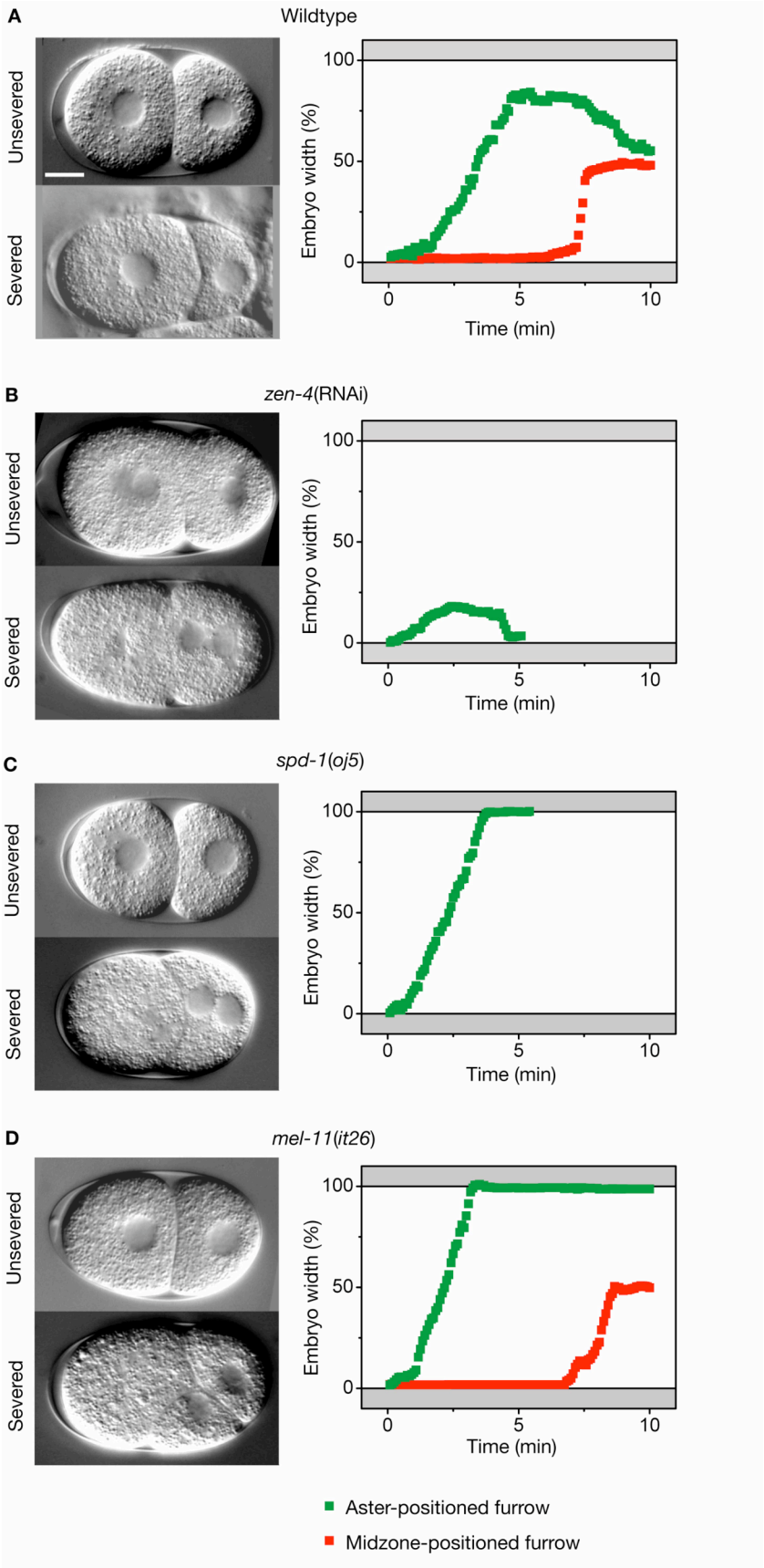
A
Wildtype
Unsevered
Severed
Embryo width (%)
100
50
0
0
5
10
Time (min)
B
zen-4(RNAi)
Unsevered
Severed
Embryo width (%)
100
50
0
0
5
10
Time (min)
C
spd-1(oj5)
Unsevered
Severed
Embryo width (%)
100
50
0
0
5
10
Time (min)
D
mel-11(it26)
Unsevered
Severed
Embryo width (%)
100
50
0
0
5
10
Time (min)
Aster-positioned furrow
Midzone-positioned furrow

Figure 9

Figure 9: The spindle midzone is dispensable for cytokinesis completion but inhibits aster-positioned cytokinesis. **A – D**, Phenotypic defects after ASS: top left is unsevered control and bottom left is severed, shown at the time the cytokinesis furrows are maximally ingressed. Right is cleavage progression plotted versus time, aster-positioned furrow is green, midzone-positioned furrow is red **A**, Wildtype, the aster-positioned furrow does not complete, but pauses. The cytokinesis furrow position is then corrected by the midzone, and part of the aster-positioned furrow regresses. **B**, Both furrowing activities are affected in *zen-4*(RNAi), leading to a failure in cytokinesis. **C**, No midzone positioned cytokinesis in *spd-1*(*oj5*)mutants: the embryo divides solely using its aster-based mechanism leading to one cell that contains no nucleus, and one that contains two. **D**, Failure to correct the aster-positioned furrow in hypercontractile *mel-11*(*it26*)mutant embryos: the aster-positioned furrow completes before the midzone-positioned furrow starts, leading to the generation of three cells.

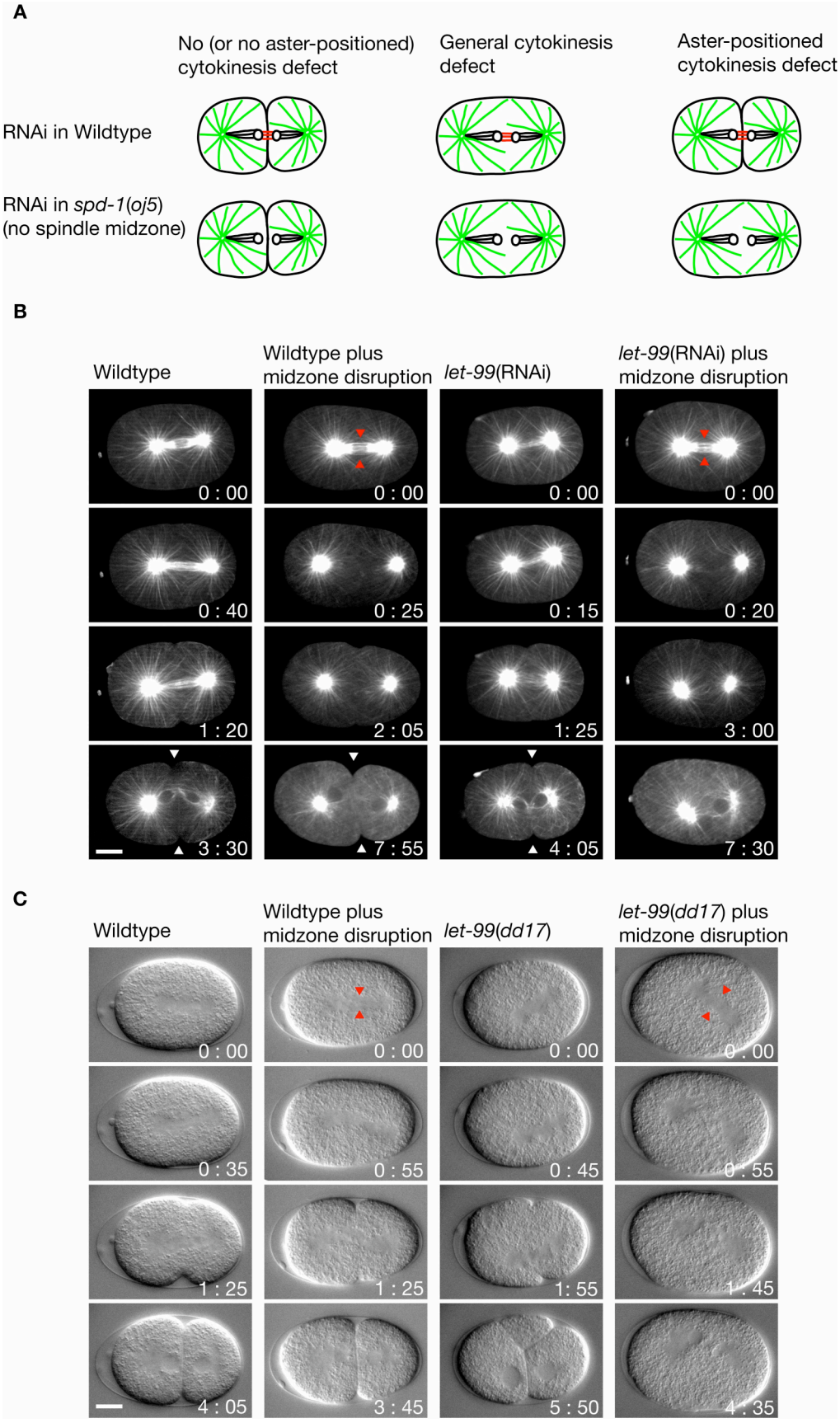
A
No (or no aster-positioned) cytokinesis defect
General cytokinesis defect
Aster-positioned cytokinesis defect
RNAi in Wildtype
RNAi in spd-1(oj5) (no spindle midzone)
B
Wildtype
Wildtype plus midzone disruption
let-99(RNAi)
let-99(RNAi) plus midzone disruption
0 : 00
0 : 40
1 : 20
3 : 30
0 : 00
0 : 25
2 : 05
7 : 55
0 : 00
0 : 15
1: 25
4 : 05
0 : 00
0 : 20
3 : 00
7 : 30
C
Wildtype
Wildtype plus midzone disruption
let-99(dd17)
let-99(dd17) plus midzone disruption
0 : 00
0 : 35
1 : 25
4 : 05
0 : 00
0 : 55
1 : 25
3 : 45
0 : 00
0 : 45
1: 55
5 : 50
0 : 00
0 : 55
1 : 45
4 : 35

Fig. 10

Figure 10: LET-99 is required for aster-positioned cytokinesis **A** Cartoon description of the *spd-1* screen. *Spd-1* embryos don't form a spindle midzone and cleave using aster-positioned cytokinesis. RNAi leading only to a defect in aster-positioned cytokinesis should allow cleavage in wildtype embryos but result in cytokinesis failure in *spd-1* embryos. **B** Mechanical spindle midzone disruption in *let-99*(RNAi) using a UV laser observed in tubulin fluorescence using spinning disk microscopy. **C** Mechanical spindle midzone disruption in *let-99*(*dd17*) mutant embryos using a UV laser observed in DIC optics. Red arrows indicate the irradiated region. Scale is 10 μm. Time is min : sec.

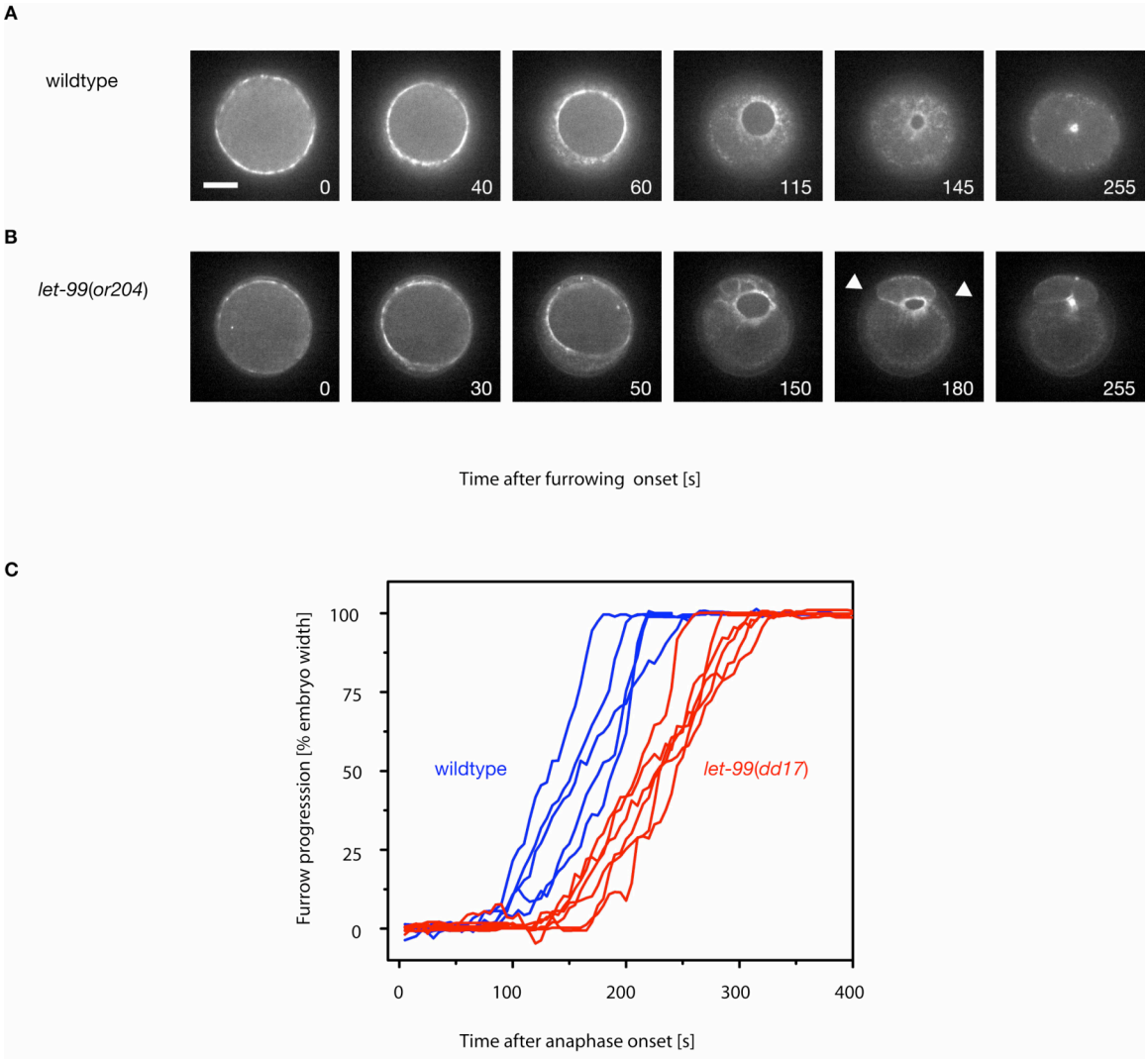

Figure 11: LET-99 is required to organize the contractile ring. **A-B** Contractile ring in wildtype **A** and *let-99*(*or204ts*) mutant **B** embryos visualized by NMY-2::GFP using spinning-disk microscopy. Time is seconds. Scale bar is 5µm. **C** Kinetics of furrow ingression. Plotted is furrow progression (% embryo diameter) vs. time (s). Shown are wildtype (blue) and *let-99*(*dd17*) (red).

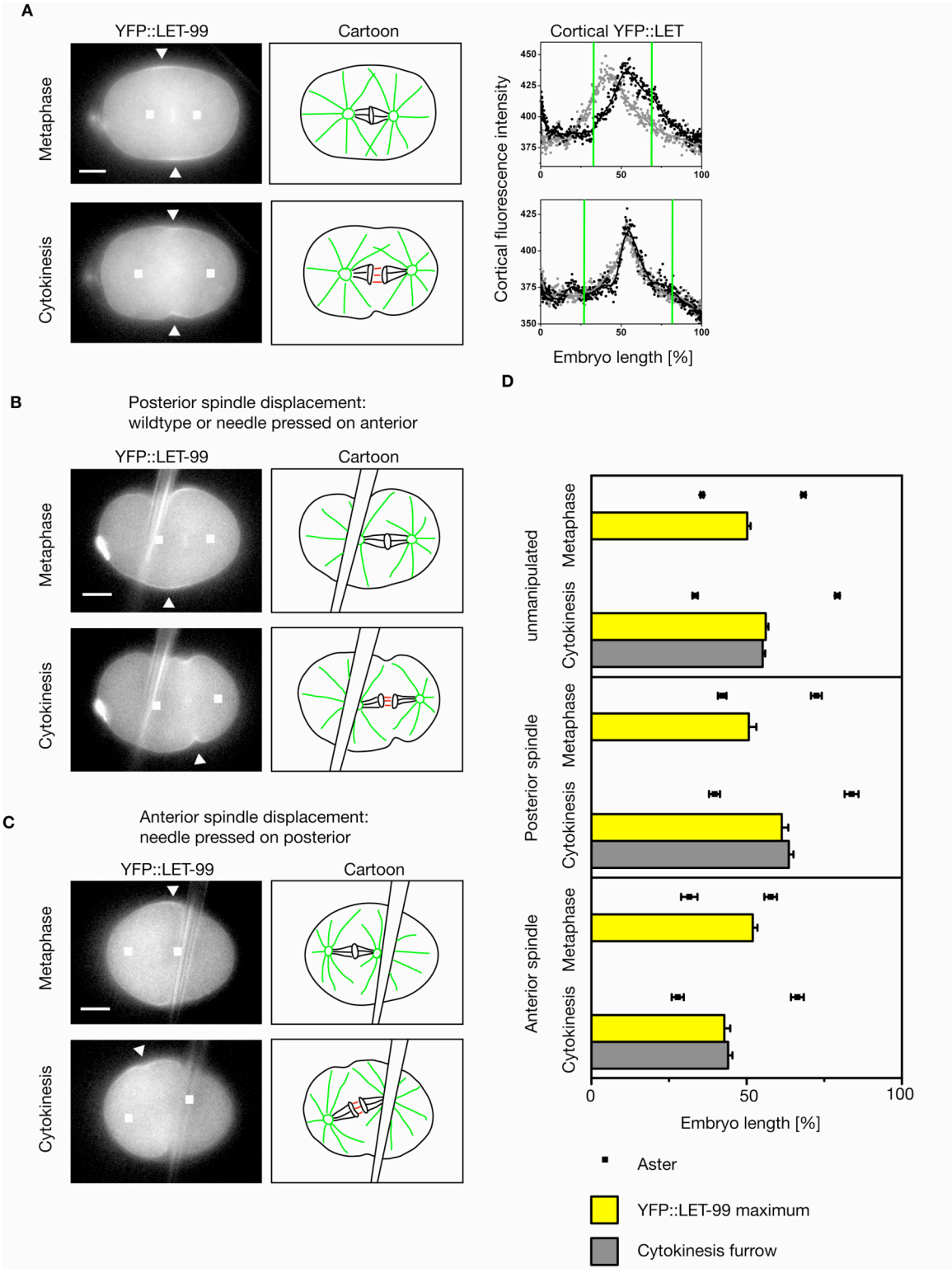
A
YFP::LET-99
Cartoon
Metaphase
Cytokinesis
Cortical YFP::LET
Cortical fluorescence intensity
Embryo length [%]
B
Posterior spindle displacement:
wildtype or needle pressed on anterior
C
Anterior spindle displacement:
needle pressed on posterior
D
unmanipulated
Posterior spindle
Anterior spindle
Aster
YFP::LET-99 maximum
Cytokinesis furrow

Figure 12

Figure 12: The mitotic spindle positions cortical LET-99 at anaphase/cytokinesis but not at metaphase. **A** LET-99 localization. Shown is YFP::LET-99 epifluorescence during metaphase (top) and cytokinesis (bottom). White squares and cartoon indicate position of aster centers, arrowheads indicate the peak of cortical LET-99. Scale bar is 10μm. LET-99 localizes to the cortex, the polar body, metaphase chromosomes and the spindle midzone. Plots display cortical fluorescence intensity vs. embryo length. Anterior is to the left, posterior is to the right. Cartoons show the position of the mitotic spindle. Astral microtubules are indicated in green, spindle midzone microtubules are indicated in red. **B-C** Spindle displacement assay. **B** A glass needle is pressed on the anterior of the cell. The spindle is hyperdisplaced to the posterior compared with wildtype embryos. **C** A glass needle is pressed on the posterior of the cell. The spindle is displaced to the anterior of the cell. Shown are YFP::LET-99 fluorescence during metaphase and cytokinesis. White squares and cartoon indicate position of aster centers, arrowheads indicate cortical LET-99. Scale bar is 10μm. Errors are SEM. Cartoons show the position of the needle and the mitotic spindle. Astral microtubules are indicated in green, spindle midzone microtubules are indicated in red. **D** Quantification of spindle displacement. The peak of LET-99 intensity is in the middle of the embryo at metaphase, regardless of spindle position, but shifts to the position midway between the asters at anaphase/cytokinesis. Black squares are aster centers. Yellow histogram is YFP::LET-99 peak maximum position and grey histogram is cytokinesis furrow position. Errors are SEM.

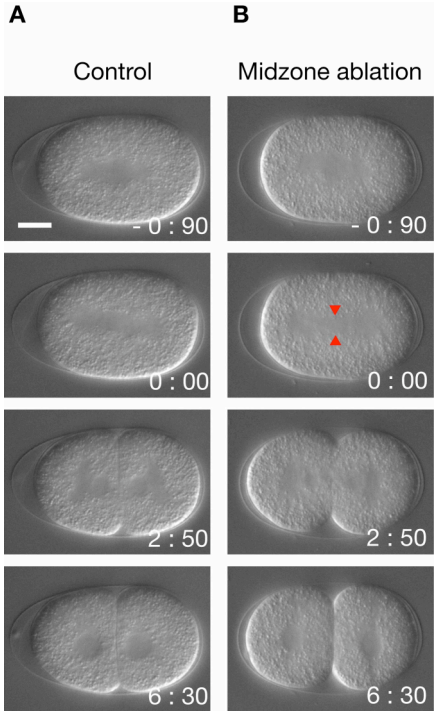

Figure 13: UV-mediated midzone ablation in polarity defective embryos does not cause a cytokinesis failure. *par-3*(*it71*) is likely a null allele and shows defective cortical polarity. **A** Control *par-3*(*it71*) embryos. **B** The spindle midzone was ablated in *par-3*(*it71*) embryos using a UV laser. Shown are DIC images, scale is 10µm. Time is minutes:seconds.

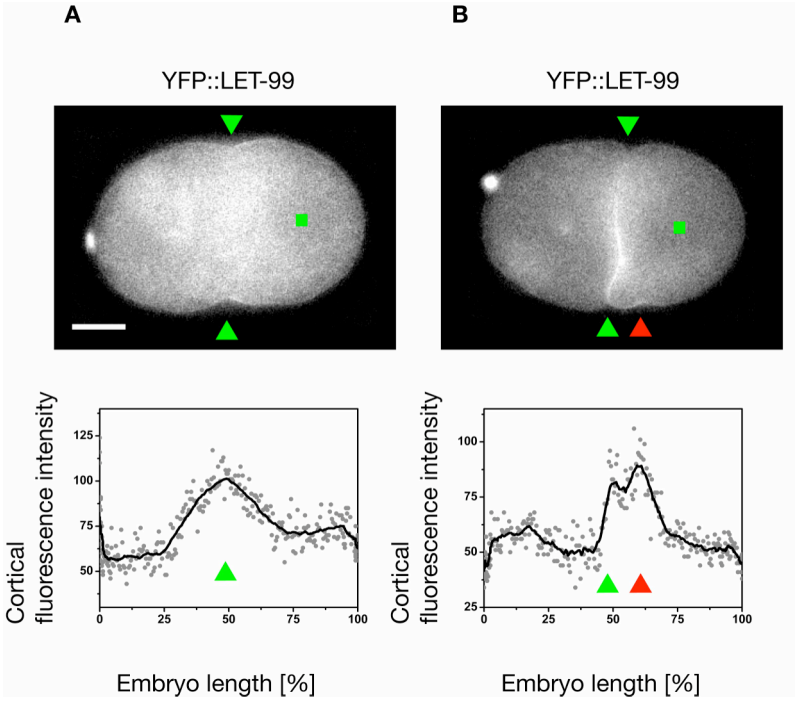

Figure 14: LET-99 localizes to both the aster-positioned furrow and the midzone-positioned furrow after ASS plus ablation of the anterior aster. Shown are (A) an embryo at the time of aster-positioned furrow formation following ASS and (B) an embryo at the time of midzone-positioned furrow formation following ASS. Green arrows indicate the aster-positioned furrow, the red arrow indicates the midzone-positioned furrow. Green boxes indicate aster positions. Scale bar is 10µm. Plots show cortical YFP::LET-99fluorescence intensity vs. embryo length.

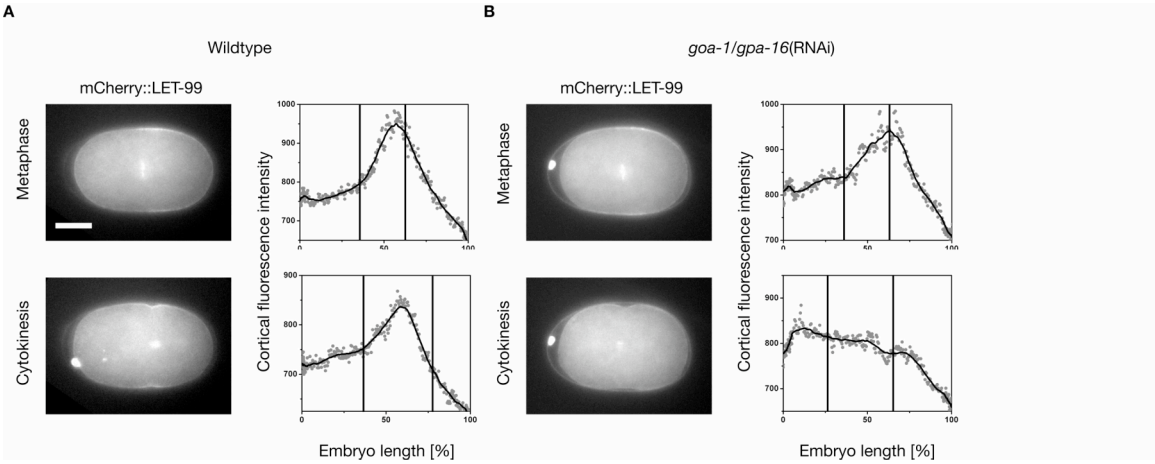

Figure 15: GOA-1/GPA-16 are required for the localization of LET-99 to the cytokinesis furrow. **A-B** LET-99 localization in wildtype **A** and *goa-1/gpa-16*(RNAi) **B**. Shown is mCherry::LET-99 epifluorescence during metaphase (top) and cytokinesis (bottom). Scale bar is 10µm. Plots display cortical mCherry::LET-99 fluorescence intensity vs embryo length. Vertical bars indicate aster position. Anterior is to the left, posterior is to the right.

Final Discussion

What are the relative contributions of microtubule asters and the spindle midzone?

Microtubule asters and the spindle midzone are both implicated in cytokinesis. The classic way to analyse the role of different spindle parts is to remove parts of the spindle and test whether the remaining parts are sufficient for cytokinesis. Such studies have concluded that asters alone, the spindle midzone alone and even a bundle of microtubules can induce a furrow. The results suggested that either microtubule asters or the spindle midzone alone might be used by a particular system induce a furrow, but the idea that both structures might act together was often neglected. These studies were carried out in different organisms and cell types, and thus it was difficult to discern a conserved mechanism by which the cytokinesis furrow is positioned. However, there was evidence that both the asters and the midzone might play a role in cytokinesis in early *C. elegans* embryos. Thus, *C. elegans* was a promising system to study the relative contributions of the different spindle parts together in one cell.

My analysis of the relative contributions of microtubule asters and the spindle midzone to cytokinesis was made possible by spatially separating the region midway between the asters and the spindle midzone using asymmetric severing of the mitotic spindle using a UV laser. Asymmetric spindle severing demonstrated that the cytokinesis furrow is positioned by two consecutive signals: the first signal provided by microtubule asters, and the second signal provided by the spindle midzone. Classic work has shown that a furrow, once initiated, can cleave a cell without further need of a spindle. If either

the asters or the midzone alone can induce a furrow, it seems reasonable to assume that either the asters or the midzone alone should be able to cleave the cell.

Is redundant furrow positioning a conserved principle?

I carried out my experiments in the early *C. elegans* embryo. But what are the relative contributions of asters and the midzone in other systems? Early blastomeres, such as sea urchin or salamander eggs, have relatively small spindles, and thus small spindle midzones, but big asters. Differentiated cells in some tissues and tissue culture cells have relatively big spindles, and thus big spindle midzones, but small asters [6]. The variation in the relative size of asters and midzone suggests that the relative contributions of asters and midzone to cytokinesis furrow positioning might differ among cell types. Although one of the two pathways may be dominant in certain cell types or organisms, it seems most likely that a spindle composed of asters and a midzone would use both structures to position the cytokinesis furrow. It would be interesting to perform ASS in different cell types to analyse potential differences in the relative contribution to cytokinesis furrow formation in different systems and to see if such differences correlate with the sizes of the midzone and asters relative to the cell.

Why are there two cytokinesis signals?

If both the asters alone and the spindle mizone alone can cleave the cell, then why does the cell use two redundant mechanisms? In

theory such questions can be addressed in experiments that inhibit either aster-positioned cytokinesis or midzone-positioned cytokinesis. In this study, midzone-positioned cytokinesis was prevented by ablation of the spindle midzone. The ablation was made either genetically using the *spd-1*(*oj5*) mutant or mechanically using a UV laser. Aster-positioned cytokinesis can be removed genetically using LET-99 depletion. Theoretically, the asters could be removed mechanically, for instance using a UV laser. However, I was not able to establish a way to reproducibly ablate the asters.

The role of the asters

In the absence of LET-99, cytokinesis is defective: The contractile ring forms later, is irregularly shaped, and ectopic furrowing occurs. The results suggest that aster-positioned cytokinesis is important, at least in early embryos. Microtubule asters directly touch the cortex. Thus they may be able to deliver a cytokinesis signal faster than the midzone, which is buried in the center of the cell. By directly touching the cortex, the signal may also be more homogenous, leading to the formation of a more regular ring. The spindle midzone is thought to deliver a positive signal in its vicinity. The aster could deliver a positive but also a negative signal to the cortex. The role for a negative signal could be to avoid ectopic furrowing.

Alternative explanations of the LET-99 depletion phenotype are also possible. For instance, it is possible that the aster-dependent signal does not improve the fidelity of cytokinesis but rather that LET-99 has a non-essential role in midzone-positioned cytokinesis. Again, the role of LET-99 in midzone-positioned furrowing, would be to

increase the speed and precision of contractile ring formation and to prevent ectopic furrowing.

To try to determine whether LET-99 specifically acts in aster-positioned cytokinesis, I tried to analyse the relative contributions of the asters and the midzone in LET-99 depleted embryos using ASS. Unfortunately ASS analysis was not possible. Several reasons might have caused ASS analysis to fail in such embryos. After ASS in both wildtype and LET-99 depleted embryos, asters initially move apart due to cortical pulling forces. In wild-type embryos, the asters stay apart and the cytokinesis furrow forms midway between them. Spindle geometry remains asymmetric. In LET-99 depleted embryos, the asters quickly move back together, thereby restoring the original symmetric spindle geometry before any signs of contractile ring assembly or cytokinesis furrow formation (data not shown). Increasing astral pulling forces using PAR-3 depletion did not solve this problem. It would be interesting to modify the ASS assay so that it can be used to analyse the relative contributions of microtubule asters and the spindle midzone in LET-99 depleted embryos. It might be possible to keep the two asters apart after ASS using optical tweezers or microneedles. Additionally, to better assess the specific role of aster-positioned cytokinesis, it would be ideal to analyze cytokinesis in the absence of astral microtubules, for instance using cells with mechanically removed asters. Such experiments would also help resolve whether the defects observed in *let-99* mutants are specific to the aster-dependent signal.

The role of the midzone

In the absence of a spindle midzone, cytokinesis appears relatively normal, although the cells cleave slightly faster than in the presence of a spindle midzone. A severe defect in embryos lacking a spindle midzone was only seen after ASS; one daughter cell contained both nuclei, the other cell contained no nuclei. Such a condition is most likely lethal. Wildtype cells can develop into adult worms after ASS. Do ASS-like perturbations occur in the normal life of *C. elegans*? *C. elegans* is a soil nematode and it is possible that worms or eggs can be mechanically deformed in their natural environment – for instance, eggs could get squashed between two stones - leading to a condition in which aster-positioned furrowing alone may not be sufficient to segregate the two nuclei faithfully into two daughter cells. Alternative explanations for the role of redundant pathways are possible: as discussed above, different cell types may use aster-positioned cytokinesis and midzone-positioned cytokinesis to different extents. If cells used only one pathway, it would become essential.

Do microtubule asters and the spindle midzone use different mechanisms to position the cytokinesis furrow?

A microtubule aster is an array of radial microtubules. The microtubules touch the cortex directly. The aster-positioned cytokinesis signal is likely to involve direct microtubule-cortex interactions. The spindle midzone is an array of bundled microtubules located in the center of the cell. The midzone-positioned cytokinesis signal thus is likely to involve transduction from the spindle midzone to the cortex, a distance of about 12µm in *C. elegans* one-cell embryos. These observations suggest that

microtubule asters and the spindle midzone use different mechanisms to induce a cytokinesis furrow. Evidence for the different mechanisms used by the two types of cytokinesis furrow positioning is the existence of molecules that are specifically required for one of the two pathways, in other words, the finding that a molecule is required for one pathway but dispensable for the other. LET-99 and the G proteins are such molecules. They are specifically required for aster-positioned cytokinesis.

How do microtubule asters provide spatial information to position the cytokinesis furrow?

Microtubule asters and the spindle midzone appear to use different mechanisms to induce the cytokinesis furrow. What is the nature of the furrow-positioning signal, and specifically, how is spatial information transmitted to the cortex? My work focused mainly on aster-positioned cytokinesis. Thus, I will not speculate about the mechanism the spindle midzone uses to position and induce a furrow. Instead, I would like to put forward a hypothetical model for aster-positioned cytokinesis. To my knowledge this model does not exist in the literature.

The signal for aster-positioned cytokinesis is likely to involve direct mictotubule-cortex interactions. What is the nature of the interaction of microtubules and the cortex? Interactions between microtubule asters and the actomyosin cortex are not only important for cytokinesis furrow positioning but also play a role in positioning the mitotic spindle: At metaphase, the spindle is positioned roughly in the center of the cell. At anaphase, the spindle is slightly displaced to the posterior. The position of the spindle within the cell depends on the actomyosin cortex and on microtubules: it is thought that cortical

force generators that contact and pull on astral microtubules determine the position of the spindle. A symmetric distribution of force generators leads to centration of the spindle, while an asymmetric distribution of force generators leads to displacement of the spindle away from the center. At anaphase, more force generators on the posterior cortex are pulling on microtubules compared to the anterior cortex, leading to a posterior spindle movement. The clearest demonstration that pulling forces act on microtubule asters is that asters move apart rapidly after cutting the spindle into two half-spindles using a UV laser[37]. LET-99 and the G proteins have been implicated in regulating the cortical pulling forces that act on microtubules[46]. The requirement of LET-99 and G proteins for aster-positioned cytokinesis might suggest a role for astral microtubule-dependent pulling forces during aster-positioned cytokinesis. It is possible that microtubule-based pulling forces provide a mechanical signal to the cortex to position a furrow. How could pulling act as a spatial signal for furrow positioning? Microtubules contact the cortex at different angles. Microtubules pulling on the cortex would generate lateral forces on the cortex that depend on the angle. See the cartoon in figure 16. Spatial differences in the lateral force strength could generate a mechanical signal, for instance, by creating a change in cortical tension. Because of the geometry of astral microtubule-cortex contacts, my model predicts that lateral cortical tension would be highest between the asters. See figure 15.

This model also predicts the existence of a mechanosensing pathway that can respond to lateral cortical force/tension, for example. LET-99 may be part of this mechanosensing pathway. LET-99 could recognize the region of highest tension, subsequently leading to the

assembly of contractile ring components. Contractile ring assembly would further increase the cortical tension, which would further activate the mechanosensing pathway and generate a feedback loop, eventually leading to cytokinesis furrow ingression. If any furrow generates lateral cortical tension, and if LET-99 localizes to the region of highest tension, this model would predict that LET-99 would localize to any furrow, including the midzone-positioned furrow. Consistent with this model, LET-99 indeed localized to the midzone-positioned furrow. Previous models of aster-positioned cytokinesis furrow specification proposed that the cortex responds to inhomogeneity in delivery of the astral signal to the cortex. My model suggests that mechanical force inhomogeneity within the cortex generated by non-uniform pulling forces is the primary signal driving aster-dependent cytokinesis. Inhomogeneity would be caused by microtubules touching the cortex with different angles. Further work is needed to test this model.

Figure Final Discussion

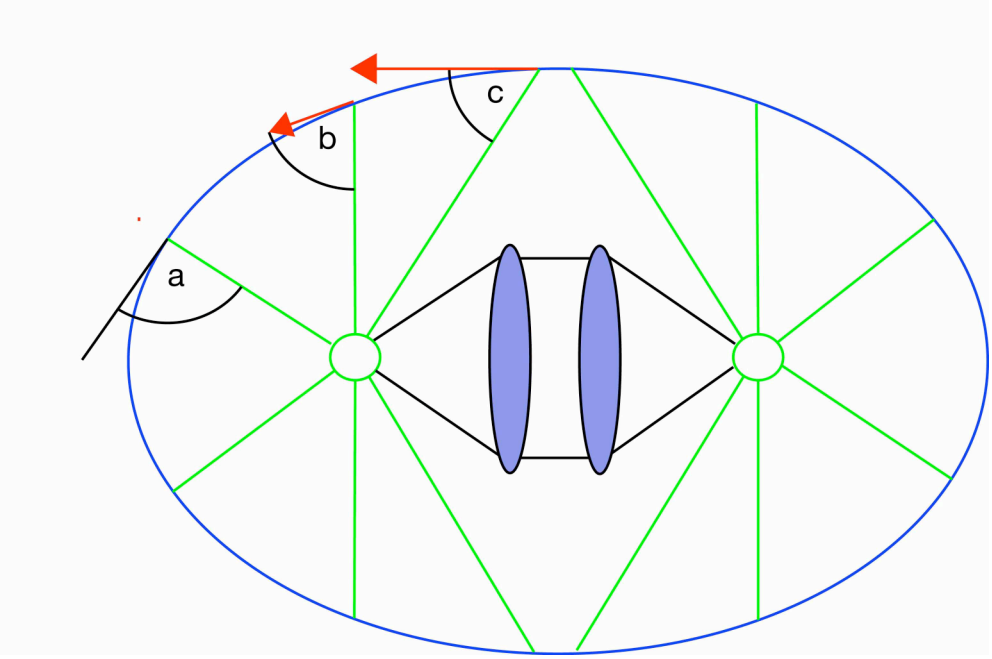

Figure 15: Hypothetical model for aster-positioned cytokinesis. Astral microtubule (green) pull on the cortex (blue) causing lateral cortical forces (red arrows) that depend on the angle at which the microtubules contact the cortex (a-b are the different angles, a > b > c, the red arrows indicate lateral cortical force). These lateral cortical forces could act as a signal for cytokinesis cleavage plane positioning.

Abbreviations used

ASS	asymmetric spindle severing
YFP	Yellow Fluorescent Protein
GFP	Green Fluorescent Protein
UV	ultraviolet

Supplementary information

All supplementary information can be found in the CD at the end of the thesis.

Supplementary movies

Supplementary movie 1
This movie shows a *C. elegans* zygote at the metaphase-to-anaphase transition. Note the displacement of the spindle toward the posterior (right) and the disappearance of the metaphase plate at anaphase onset.

Supplementary movie 2
This movie shows asymmetric spindle severing (ASS): the anterior centrosome (left) is chopped off. The position and time of laser ablation is marked with a white circle.

Supplementary movie 3
This movie shows cytokinesis in an unsevered control *C. elegans* zygote.

Supplementary movie 4
This movie shows cytokinesis following anterior ASS: Note the formation of two distinct furrows after ASS. The severed region is highlighted with a grey bar. The first furrow does not complete, but pauses and then regresses.

Supplementary movie 5

This movie shows cytokinesis following posterior ASS: Note the furrow correction observed after ASS. The cut region is highlighted with a grey bar. The focus is rapidly changed during the correction process to reveal the position of the nuclei and the complexity of the cytokinesis furrow.

Supplementary movie 6

This movie shows ASS with subsequent disintegration of the chopped-off aster. The time and place of laser ablation is marked with a white circle.

Supplementary movie 7

This movie shows cytokinesis following ASS with disintegration of the chopped-off aster. The posterior centrosome (highlighted with a white circle) is chopped off and disintegrated. The frames during which the aster was disintegrated were removed (see movie 6 for details of the disintegration assay). Note that the first furrow sets up further away from the remaining aster compared with wildtype or conventional ASS.

Supplementary movie 8

This movie shows cytokinesis in a *zen-4*(RNAi) one-cell embryo. Note that the spindle snaps at anaphase. The furrow regresses and cytokinesis fails.

Supplementary movie 9

This movie shows cytokinesis following ASS in a *zen-4*(RNAi) embryo. The severed region is highlighted with a grey bar. The

posterior aster is chopped off. Note that the ingression of the first furrow is reduced compared with wildtype (movie 4).

Supplementary movie 10
This movie shows cytokinesis in a *klp-7*(RNAi) zygote. Note that the spindle snaps at anaphase.

Supplementary movie 11
This movie shows cytokinesis following posterior ASS in a *klp-7*(RNAi) zygote. The severed region is highlighted with a grey bar.

Supplementary movie 12
This movie shows cytokinesis in a *mel-11*(it26) mutant zygote.

Supplementary movie 13
This movie shows cytokinesis following posterior ASS in a *mel-11*(it26) mutant zygote. The severed region is highlighted with a grey bar. Note that the aster-dependent furrow completes before the midzone-dependent furrow appears, leading to the formation of three cells. The furrow that separates the anterior aster from the anterior nucleus was not stable and regressed (not part of the movie).

Supplementary movie 14
This movie shows cytokinesis in a wildtype *C. elegans* one-cell embryo observed by DIC microscopy.

Supplementary movie 15

This movie shows cytokinesis in a wildtype *C. elegans* one-cell embryo observed by DIC microscopy. The spindle midzone is ablated using a UV laser.

Supplementary movie 16
This movie shows cytokinesis in a *let-99*(*dd17*) *C. elegans* one-cell embryo observed by DIC microscopy.

Supplementary movie 17
This movie shows cytokinesis in a *let-99*(*dd17*) *C. elegans* one-cell embryo observed by DIC microscopy. The spindle midzone is ablated using a UV laser.

Supplementary movie 18
This movie shows mechanical spindle displacement using a glass needle observed in DIC microscopy.

Supplementary table

Set of 1021 genes that produce an embryonic lethal phenotype used for the *spd-1(oj5)* screen. The table indicates whether the feeding clone produced multinucleated cells in *spd-1(oj5)* or wildtype worms, and whether the multinucleated phenotype was caused by a failure in cytokinesis. The gene set contained feeding clones that our lab had already ordered before the screen plus all genes that have been reported to produce an embryonic lethal phenotype. The set is incomplete compared with the screens mentioned above because not all of the clones requested from MRC Geneservice could be obtained. I sequenced 100 feeding clones of this library and 87% were correct.

Materials and Methods

Worm culture

Worms were cultured on NGM plates and fed OP50 bacteria as described[49]. The media kitchen and Andrea Zinke prepared all plates (Susanne Ernst prepares the plates). All strains were maintained at 16°C. Temperature-sensitive strains and strains expressing transgenes were shifted to 25°C for 24h before an experiment.

RNAi

RNAi was performed either using injection of double stranded RNA or by feeding, as described[19, 21]. After injections, worms were incubated at 16°C or 25°C and analysed 48 and 24 h after injection. For feeding experiments worms were incubated at 16°C or 25°C for 48 or 72 hours. Worms were mated with males to maintain egg laying.

For *let-99*(RNAi) experiments RNAi-by-injection was used. Genomic DNA was used as a template to make the *let-99* double stranded RNA. I injected the RNA at a concentration of 1µg/µl into the gonads of young adult hermaphrodites. *let-99* RNA was produced using the primers TAATACGACTCACTATAGGCAAGGCTCCCACGAAGATTA and AATTAACCCTCACTAAAGGCGCAGACGAAGAAATCATCA.

For *zen-4*(RNAi) and *goa-1/gpa-16*(RNAi), RNAi-by-feeding was used as described. The *zen-4* feeding clone was a gift from Michael Glotzer and Michael Werner, the *goa-1/gpa-16* feeding clone was a gift from Pierre Gonczy and Katy Afshar.

RNAi-by-feeding screening

Bacterial feeding strains were obtained from MRC Geneservice in 96 well plates. Plates were thawed and starter cultures were inoculated using a 96 well replicator (Boekel)(1.2ml LB, containing 0.1mg/ml ampicillin and 12.5 µg/ml tetracyclin, in 96 deep well plates). The starter cultures were incubated at 37°C overnight on a high-speed shaker (600rpm). A fresh culture (LB, amp) was inoculated using a replicator and grown for 6-7 h at 37°C again on a high-speed shaker. Then IPTG was added to a concentration of 3µM and 200 µl of the culture was spread onto plates containing NGM plus 1mM IPTG and 25µg/ml carbenicillin (6cm diameter). Plates were dried and incubated at 20°C for approx. 12 h. A synchronized population of L3 worms was generated starved plates: worms were transferred from starved plates to NGM plates containing bacteria and incubated 40h at 16°C. The worms were washed off the plates with M9 plus gelatin (0.25%) and were collected using centrifugation. The worms were washed by repeated resuspension in M9 plus gelatin and collection by centrifugation. The concentration of the worms was adjusted empirically to 10 worms per 20 µl. Worms were aliquoted onto the plates so that each plate contained 5-15 worms. The plates were incubated at 16°C for 24H and then shifted to 25°C for 24h. The

worms were dissected and mounted on an agarose pad and visually inspected using DIC optics and a 40x dry lens

Generation of *let-99* deletion alleles

The *let-99(dd17)* deletion allele was generated using EMS mutagenesis and isolated using PCR screening as described[50]. Alex Tudor Constantinescu, Joanne Stamford and other people of the Christian Eckmann lab constructed the deletion library. The library consisted of about one million mutagenized genomes and was provided as 100 pools of 10 000 genomes each. The mutant allele was identified in one of the pools using nested PCR using the primers CGCAGAGAAGGAGTCATTGG plus CGGAGTTCGTTGTTTCTTCG (outer) and GTAAACGGCGAAAAGAGCAG plus ACGCCGCCTGAAGAATTATC (inner). The pool was subsequently split into subpools that each constisted of one tenth of the original pool. The pools were split up until a population was identified that was generated by one worms containing the mutation. The deletion was backcrossed five times into wildtype N2 and followed again by PCR. The deletion was maternal effect lethal and was balanced using nT1 GFP. Our sequencing facility sequenced the mutant product. *Let-99*(*dd17*) contains a 647bp deletion with the flanking sequences AATTTTTAGGAAGTTTCCAGAAATTTTTCC / CAAGGCTCCCACGAAGATTATCGCGATCTA. The deletion removes the N terminus of the open reading frame including the start codon and the DEP domain. Thus the allele likely is a null allele.

Using the same procedure I also isolated an additional allele, *let-99*(*dd19*), using the outer primers GGTGTGGTAGACTTCTCATCG and CGTCGTCGATACTTTGAAGC and the inner primers AGAATCCAGTACCAGGCAAC and GAAGATCACGGGAGAATCC. *Let-99*(*dd18*) contains a 1039bp deletion with the flanking sequences TTTGGATGAGTTGAAGCATCCCAAGCCCCG / ATGAATGCTCTCTTATTGTTAATCTCCTCT. The deletion starts behind the DEP domain. I did not further characterize *let-99*(*dd18*) but concentrated my analysis on *let-99*(*dd17*)

Generation of strains expressing fluorescent protein::LET-99 fusion constructs:

These constructs were all made and tested for functionality by Jun Kong as part of his master thesis under my supervision. The *let-99* gene was PCR amplified from genomic DNA using the primers GGCCACTAGTGGAGGAGGAATGTCTGCCGACTACTCATCG and GGCCCCCGGGTTATTTACGCAGCAATCTTGTGAA and was cloned into paz(N)YFP using XmaI and SpeI. The construct was sequenced and no mutations were found. The construct was bombarded into *unc-119(ed3)* mutant worms and transgene worms were selected based on *unc-119* rescue. To generate mCherry::LET-99, the YFP coding region was cut out from the paz(N)YFP::LET-99 plasmid using PacI and SpeI and the mCherry coding was cut out using the same restriction sites, ligated into the vector to replace the YFP.

Functionality tests for LET-99 fusion constructs

To test for functionality, YFP::LET-99 was crossed into the mutants *let-99*(*or204ts*) and *let-99*(*or81*). Both mutants produce almost 100% lethality. Hatch rates were 95% (326/344), 45% (196/431) and 43% (180/419) for YFP::LET-99, YFP::LET-99;*let-99*(*or81*), and YFP::LET-99;*let-99*(*or204ts*) embryos. The rescued embryos displayed a mild *let-99* mutant phenotype, including incomplete spindle centration and lack of spindle rotation in P1 (data not shown). Thus, the construct partially rescued the lethality and mutant phenotype. The functionality of mCherry::LET-99 was tested by directly bombarding the DNA construct into *let-99*(*or81*);*unc-119*(*ed3*) mutant worms. *Let-99*(*or81*) was balanced using nT1 with a Pharynx GFP marker to identify homozygous mutant worms (nongreen). A viable homozygous *let-99*(*or81*) line was isolated that showed *unc-119* rescue (hatch rates for homozygous *let-99*(*or81*) worms was 0.4% (1/229) before transformation with mCherry::LET-99 and 70% (90/128) after transformation with mCherry::LET-99. RNAi of mCherry caused inviability in homozygous *let-99*(*or81*);mCherry::LET-99 but not in mCherry::LET-99 embryos. The hatch rate after mCherry(RNAi) was 2.9% (5/173) for mCherry::LET-99;*let-99*(*or81*) and 93 % (214/229) for mCherry::LET-99.

Microscopy

All imaging was carried out on an Axiovert 200M, Zeiss as described [38]. The lense used was Apochromat (Zeiss), 63x NA 0.17, water. Fluochromes used for epifluorescence were eGFP, YFP and

mCherry. We used Zeiss filter sets No. 10 (exitation 450-490nm, emission 515-565nm, beamsplitter 510nm) for GFP, No. 46 (exitation 490-510nm, emission 520-550nm, beamsplitter 515nm)for YFP and filter set 45 (exitation 540-580nm, emission 595-670nm, beamsplitter 585nm) for mCherry. For spinning disk imaging I used a Melles Griot ArIon Laser (488nm, 100mW). A Hamamatsu Orca-ER, controlled by metamorph software or CCC software, was used for image acquisition. 2x binning was used for epifluorescence imaging. Embryos were mounted on 2% agarose pads in M9 except if mechanical manipulations were carried out using a glass needle (compare end-on view and mechanical spindle displacement).

Image processing and quantification

Images for display figures were processed in Photoshop (adobe). Images were rotated and cut. Levels and contrast were manually adjusted. Movies were generated in quicktime format using Metamorph. To quantify cortical fluorescence intensity images were rotated so that their long axis aligned on the x axis. A line was drawn manually along the cortex starting at the anterior pole and ending at the posterior pole. The polar body was not counted as part of the embryo. A linescan was produced using metamoph software, line width was 9 pixels and maximum intensity was measured along the line for all points (x,y) on the line. To project the intensity onto the long axis of the embryo the y value was discarded. The first point was defined as 0% embryo length and the last point was defined 100% embryo length. Data were plotted using origin 7 software. Data were averaged over 30 points to smoothen the curve. Both the

original data points and the averaged line are shown in the plots. Peak maxima for YFP::LET-99 could be clearly determined for all cases (20/20), but beginning and starting points of the peak were only clearly visible in some (16/20) cortices due to background fluctuations. I thus found measuring the peak position maximum more useful than measuring beginning and end of the peak.

UV laser experiments

Laser setup

The laser ablation experiments were performed using a highly focused ultraviolet (wavelenth 354nm) laser (Nd:YAG, Powerchip, JDS uniphase) as described in[38]. All ablations were performed in DIC optics. For some cases fluorescence imaging was used before and/or after the ablation.

Asymmetric spindle severing (ASS)

The ASS was performed just after anaphase onset, identified by the disappearance of the metaphase plate, observed in DIC microscopy. At the time of the spindle severing spindle midzone components like ZEN-4 are already localized to the spindle midzone (my unpublished observations using ZEN-4::GFP). Five to ten shots at 250 Hz / 25 pulses were taken at the region midway between one aster centre and the separated chromatin. If the same number of shots was fired in the region between spindle and cortex, no severing of the spindle is observed (data not shown). The position of the first furrow was measured at the time it had ingressed roughly two thirds of egg

width. The position of the second furrow was measured at the initial time the furrow was visible. If the furrow showed bent growth, I measured the final position the furrow was aiming at. The position of the final furrow was measured at the time the two blastomeres rounded up and the furrow was perpendicular to the anterior-posterior axis of the embryo. For furrow trackings, I focused such that the largest opening was visible. I compared the tracking data collected in DIC or fluorescence mode of an NMY-2::GFP embryo and obtained comparable results. For simplicity, DIC movies were used for all quantifications. After ASS, the aster-positioned furrow is usually unilateral in wildtype embryos but bilateral in MEL-11 and SPD-1 embryos, which accounts for the different cytokinesis progression speeds.

Aster ablation

In order to ablate the asters, 15 to 20 additional shots were delivered in the centre of the aster (the region devoid of yolk granules) after it had been chopped off. The stage was rapidly moved in circles around the centre of the aster during shooting to prevent spreading of the aster fragments. Distributing the shots in the astral region that contained yolk granules left the aster intact and the first furrow was not displaced (data not shown). Optical sections were taken with a spinning-disk microscope. I zoomed through the embryo to verify the absence of the aster. Furrow positions were quantified as for ASS for five embryos. I observed the cell containing the irradiated aster for the time equivalent to several additional cell division cycles using DIC and spinning disk microscopy and could not find any sign of an aster reforming.

Laser-mediated midzone ablation

To ablate the spindle midzone 10-15 shots at a repetition rate of 250 hz were focused at the spindle midzone at anaphase, after the separation of sister chromatids was clearly visible. Spindle snapping indicated successful disruption of the spindle midzone. The two asters quickly moved to the poles of the cell. I took optical sections of the alphatubulin::YFP or ZEN-4::GFP embryos, and could not detect a midzone. I observed the embryo after the assay in both spinning disk fluorescence and in DIC optics and obtained comparable results. I also performed control ablations: the laser irradiation was aimed not at the spindle midzone but at the region between the spindle midzone and the cortex closest to the spindle midzone. *let-99*(RNAi) control ablation embryos all divided (5/5) (data not shown).

Micromanipulation experiments using a glass needle

For all experiments using a glass needle to mechanically manipulate embryos the embryos were glued onto 60x24mm glass coverslips: 1-2µl of Cell-Tac solution (0.92mg/ml, BD Bioscience) were pipetted on a coverslip. A circle with a radius of 5mm was drawn around the Cell Tac area using a PAP hydrophobic Pen (Sigma). The slides were dried at room temperature and then washed first with ethanol and then with water. After the Cell Tac slides were completely dried, a 100µl drop of Embryo Buffer (EB, 10mM Tris Cl, pH 8.5, Qiagen) were pipetted onto the area containing dried Cell Tac. A gravid hermaphrodite was cut open in a 25µl drop of EB on a glass slide using two 27G needles. An individual embryo at the stage of

pronuclear migration was selected and transferred onto the Cell Tac slide using a mouth pipette and pressed tightly onto the coverslip using an eyelash. Embryos were imaged on an Axiovert 200M (Zeiss) using DIC, epifluorecence, or spinning disk fluorescence. Embryos that were recovered after this mounting and imaging procedure developed normally into fertile adults, suggesting that the mounting and imaging procedure did not grossly disrupt *C. elegans* development. All micromanipulations were carried out using a glass needle that was controlled by a micromanipulator (Maerzhaeuser, STM-T3).

Mechanical spindle displacement.

In order to mechanically manipulate the spindle position, the embryo was rotated so that its long axis was perpendicular to the axis of the glass needle. The needle was then pressed sideways onto the embryo at an angle of 15-25° relative to the coverslip surface. All needle experiments were carried out at 23-25°C room temperature.

End-on imaging of *C. elegans* one-cell embryos.

I used a glass needle that was controlled by a micromanipulator to turn the embryo on its end, so that its posterior is facing the glass coverslip. The embryo was then imaged using spinning disk microscopy. Embryos that were recovered after imaging developed normally into fertile adults, suggesting that the mounting and imaging procedure did not grossly disrupt *C. elegans* development.

Literature

1. Alberts, B.J.A.L., Julian; Raff, Martin; Roberts, Keith; Walter, Peter (2002). Molecular Biology of the Cell.
2. Rappaport, R. (1996). Cytokinesis in Animal Cells (Cambridge: Cambridge University Press).
3. Rappaport, R. (1985). Repeated furrow formation from a single mitotic apparatus in cylindrical sand dollar eggs. J Exp Zool *234*, 167-171.
4. Rappaport, R., and Rappaport, B.N. (1985). Surface contractile activity associated with isolated asters in cylindrical sand dollar eggs. J Exp Zool *235*, 217-226.
5. Bonaccorsi, S., Giansanti, M.G., and Gatti, M. (1998). Spindle self-organization and cytokinesis during male meiosis in asterless mutants of Drosophila melanogaster. J Cell Biol *142*, 751-761.
6. Wang, Y.L. (2001). The mechanism of cytokinesis: reconsideration and reconciliation. Cell Struct Funct *26*, 633-638.
7. Glotzer, M. (2004). Cleavage furrow positioning. J Cell Biol *164*, 347-351.
8. Dechant, R., and Glotzer, M. (2003). Centrosome separation and central spindle assembly act in redundant pathways that regulate microtubule density and trigger cleavage furrow formation. Dev Cell *4*, 333-344.
9. Jantsch-Plunger, V., Gonczy, P., Romano, A., Schnabel, H., Hamill, D., Schnabel, R., Hyman, A.A., and Glotzer, M. (2000). CYK-4: A Rho family gtpase activating protein (GAP) required for central spindle formation and cytokinesis. J Cell Biol *149*, 1391-1404.
10. Raich, W.B., Moran, A.N., Rothman, J.H., and Hardin, J. (1998). Cytokinesis and midzone microtubule organization in Caenorhabditis elegans require the kinesin-like protein ZEN-4. Mol Biol Cell *9*, 2037-2049.
11. Verbrugghe, K.J., and White, J.G. (2004). SPD-1 Is Required for the Formation of the Spindle Midzone but Is Not Essential for the Completion of Cytokinesis in C. elegans Embryos. Curr Biol *14*, 1755-1760.

12. Hiramoto, Y. (1956). Cell division without mitotic apparatus in sea urchin eggs. Exp Cell Res *11*, 630-636.
13. Hiramoto, Y. (1965). Further Studies on Cell Division without Mitotic Apparatus in Sea Urchin Eggs. J Cell Biol *25*, SUPPL:161-167.
14. Yatsu, N. (1912). Observations and experiments on the ctenophore egg. I. The structure of the egg and experiments on cell division. J Coll Sci Imp Univ Tokyo *32*, 1-21.
15. White, J.G., and Borisy, G.G. (1983). On the mechanisms of cytokinesis in animal cells. J Theor Biol *101*, 289-316.
16. Canman, J.C., Cameron, L.A., Maddox, P.S., Straight, A., Tirnauer, J.S., Mitchison, T.J., Fang, G., Kapoor, T.M., and Salmon, E.D. (2003). Determining the position of the cell division plane. Nature *424*, 1074-1078.
17. Wood, W.B. (1988). Introduction to C. elegans biology. *The nematode Caenorhabditis elegans*, 1-16.
18. Consortium, C.e.S. (1998). Genome sequence of the nematode C. elegans: a platform for investigating biology. Science *282*, 2012-2018.
19. Gonczy, P., Echeverri, C., Oegema, K., Coulson, A., Jones, S.J., Copley, R.R., Duperon, J., Oegema, J., Brehm, M., Cassin, E., Hannak, E., Kirkham, M., Pichler, S., Flohrs, K., Goessen, A., Leidel, S., Alleaume, A.M., Martin, C., Ozlu, N., Bork, P., and Hyman, A.A. (2000). Functional genomic analysis of cell division in C. elegans using RNAi of genes on chromosome III. Nature *408*, 331-336.
20. Sonnichsen, B., Koski, L.B., Walsh, A., Marschall, P., Neumann, B., Brehm, M., Alleaume, A.M., Artelt, J., Bettencourt, P., Cassin, E., Hewitson, M., Holz, C., Khan, M., Lazik, S., Martin, C., Nitzsche, B., Ruer, M., Stamford, J., Winzi, M., Heinkel, R., Roder, M., Finell, J., Hantsch, H., Jones, S.J., Jones, M., Piano, F., Gunsalus, K.C., Oegema, K., Gonczy, P., Coulson, A., Hyman, A.A., and Echeverri, C.J. (2005). Full-genome RNAi profiling of early embryogenesis in Caenorhabditis elegans. Nature *434*, 462-469.
21. Kamath, R.S., Fraser, A.G., Dong, Y., Poulin, G., Durbin, R., Gotta, M., Kanapin, A., Le Bot, N., Moreno, S., Sohrmann, M., Welchman, D.P.,

Zipperlen, P., and Ahringer, J. (2003). Systematic functional analysis of the Caenorhabditis elegans genome using RNAi. Nature *421*, 231-237.

22. Fraser, A.G., Kamath, R.S., Zipperlen, P., Martinez-Campos, M., Sohrmann, M., and Ahringer, J. (2000). Functional genomic analysis of C. elegans chromosome I by systematic RNA interference. Nature *408*, 325-330.
23. Schneider, S.Q., and Bowerman, B. (2003). Cell polarity and the cytoskeleton in the Caenorhabditis elegans zygote. Annu Rev Genet *37*, 221-249.
24. Gonczy, P., Schnabel, H., Kaletta, T., Amores, A.D., Hyman, T., and Schnabel, R. (1999). Dissection of cell division processes in the one cell stage Caenorhabditis elegans embryo by mutational analysis. J Cell Biol *144*, 927-946.
25. Skop, A.R., Liu, H., Yates, J., 3rd, Meyer, B.J., and Heald, R. (2004). Dissection of the mammalian midbody proteome reveals conserved cytokinesis mechanisms. Science *305*, 61-66.
26. Glotzer, M. (2005). The molecular requirements for cytokinesis. Science *307*, 1735-1739.
27. Eggert, U.S., Mitchison, T.J., and Field, C.M. (2006). ANIMAL CYTOKINESIS: From Parts List to Mechanisms. Annu Rev Biochem *75*, 543-566.
28. Piekny, A.J., and Mains, P.E. (2002). Rho-binding kinase (LET-502) and myosin phosphatase (MEL-11) regulate cytokinesis in the early Caenorhabditis elegans embryo. J Cell Sci *115*, 2271-2282.
29. Maddox, A.S., Habermann, B., Desai, A., and Oegema, K. (2005). Distinct roles for two C. elegans anillins in the gonad and early embryo. Development *132*, 2837-2848.
30. Nguyen, T.Q., Sawa, H., Okano, H., and White, J.G. (2000). The C. elegans septin genes, unc-59 and unc-61, are required for normal postembryonic cytokineses and morphogenesis but have no essential function in embryogenesis. J Cell Sci *113 Pt 21*, 3825-3837.
31. Mishima, M., Kaitna, S., and Glotzer, M. (2002). Central spindle assembly and cytokinesis require a kinesin-like protein/RhoGAP complex with microtubule bundling activity. Dev Cell *2*, 41-54.

32. Severson, A.F., Hamill, D.R., Carter, J.C., Schumacher, J., and Bowerman, B. (2000). The aurora-related kinase AIR-2 recruits ZEN-4/CeMKLP1 to the mitotic spindle at metaphase and is required for cytokinesis. Curr Biol *10*, 1162-1171.
33. Schumacher, J.M., Golden, A., and Donovan, P.J. (1998). AIR-2: An Aurora/Ipl1-related protein kinase associated with chromosomes and midbody microtubules is required for polar body extrusion and cytokinesis in Caenorhabditis elegans embryos. J Cell Biol *143*, 1635-1646.
34. Sulston, J.E., and White, J.G. (1980). Regulation and cell autonomy during postembryonic development of Caenorhabditis elegans. Dev Biol *78*, 577-597.
35. Hyman, A.A. (1989). Centrosome movement in the early divisions of Caenorhabditis elegans: a cortical site determining centrosome position. J Cell Biol *109*, 1185-1193.
36. Cowan, C.R., and Hyman, A.A. (2004). Centrosomes direct cell polarity independently of microtubule assembly in C. elegans embryos. Nature *431*, 92-96.
37. Grill, S.W., Gonczy, P., Stelzer, E.H., and Hyman, A.A. (2001). Polarity controls forces governing asymmetric spindle positioning in the Caenorhabditis elegans embryo. Nature *409*, 630-633.
38. Grill, S.W., Howard, J., Schaffer, E., Stelzer, E.H., and Hyman, A.A. (2003). The distribution of active force generators controls mitotic spindle position. Science *301*, 518-521.
39. Priess, J.R., and Thomson, J.N. (1987). Cellular interactions in early C. elegans embryos. Cell *48*, 241-250.
40. Wood, W.B. (1991). Evidence from reversal of handedness in C. elegans embryos for early cell interactions determining cell fates. Nature *349*, 536-538.
41. Rose, L.S., and Kemphues, K. (1998). The let-99 gene is required for proper spindle orientation during cleavage of the C. elegans embryo. Development *125*, 1337-1346.
42. Tsou, M.F., Hayashi, A., DeBella, L.R., McGrath, G., and Rose, L.S. (2002). LET-99 determines spindle position and is asymmetrically

enriched in response to PAR polarity cues in C. elegans embryos. Development *129*, 4469-4481.

43. Guo, S., and Kemphues, K.J. (1996). A non-muscle myosin required for embryonic polarity in Caenorhabditis elegans. Nature *382*, 455-458.
44. Kemphues, K.J., Priess, J.R., Morton, D.G., and Cheng, N.S. (1988). Identification of genes required for cytoplasmic localization in early C. elegans embryos. Cell *52*, 311-320.
45. Cheng, N.N., Kirby, C.M., and Kemphues, K.J. (1995). Control of cleavage spindle orientation in Caenorhabditis elegans: the role of the genes par-2 and par-3. Genetics *139*, 549-559.
46. Colombo, K., Grill, S.W., Kimple, R.J., Willard, F.S., Siderovski, D.P., and Gonczy, P. (2003). Translation of polarity cues into asymmetric spindle positioning in Caenorhabditis elegans embryos. Science *300*, 1957-1961.
47. Gotta, M., Dong, Y., Peterson, Y.K., Lanier, S.M., and Ahringer, J. (2003). Asymmetrically distributed C. elegans homologs of AGS3/PINS control spindle position in the early embryo. Curr Biol *13*, 1029-1037.
48. Tsou, M.F., Hayashi, A., and Rose, L.S. (2003). LET-99 opposes Galpha/GPR signaling to generate asymmetry for spindle positioning in response to PAR and MES-1/SRC-1 signaling. Development *130*, 5717-5730.
49. Brenner, S. (1974). The genetics of Caenorhabditis elegans. Genetics *77*, 71-94.
50. Kraemer, B., Crittenden, S., Gallegos, M., Moulder, G., Barstead, R., Kimble, J., and Wickens, M. (1999). NANOS-3 and FBF proteins physically interact to control the sperm-oocyte switch in Caenorhabditis elegans. Curr Biol *9*, 1009-1018.

Declaration

I herewith declare that I have produced this paper without the prohibited assistance of third parties and without making use of aids other than those specified. Notions taken over directly or indirectly from other sources have been identified as such. This paper has not previously been presented in identical or similar form to any other German or foreign examination board.

The thesis work was conducted from 1st October 2003 to 25th August 2006 under the supervision of Prof. Dr. Anthony Hyman at the Max Planck Institute for Molecular Cell Biology and Genetics.

Dresden, 25th August 2006, Henrik Bringmann